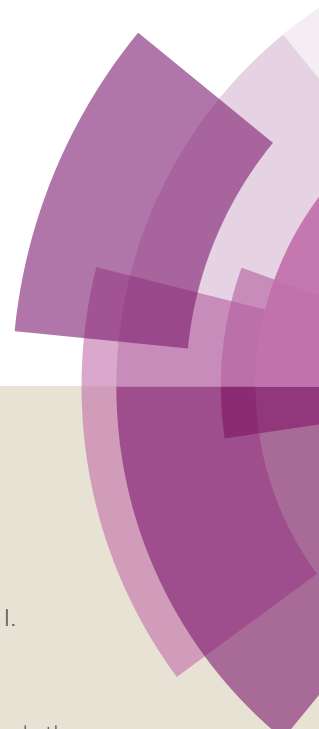


Dalton Transactions

Accepted Manuscript



This article can be cited before page numbers have been issued, to do this please use: T. S. Basu Baul, I. Longkumer, A. Duthie, P. Singh, B. Koch and M. F. C. Guedes da Silva, *Dalton Trans.*, 2017, DOI: 10.1039/C7DT04037G.



This is an Accepted Manuscript, which has been through the Royal Society of Chemistry peer review process and has been accepted for publication.

Accepted Manuscripts are published online shortly after acceptance, before technical editing, formatting and proof reading. Using this free service, authors can make their results available to the community, in citable form, before we publish the edited article. We will replace this Accepted Manuscript with the edited and formatted Advance Article as soon as it is available.

You can find more information about Accepted Manuscripts in the [author guidelines](#).

Please note that technical editing may introduce minor changes to the text and/or graphics, which may alter content. The journal's standard [Terms & Conditions](#) and the ethical guidelines, outlined in our [author and reviewer resource centre](#), still apply. In no event shall the Royal Society of Chemistry be held responsible for any errors or omissions in this Accepted Manuscript or any consequences arising from the use of any information it contains.

Triphenylstannyl((arylimino)methyl)benzoates with selective potency that induce G1 and G2/M cell cycle arrest and trigger apoptosis via ROS in human cervical cancer cells

Tushar S. Basu Baul,^{*a} Imliwati Longkumer, Andrew Duthie,^b Priya Singh,^c Biplob Koch,^{*c}
M. Fátima C. Guedes da Silva,^{*d}

Abstract

Metal complexes with organelle specificity and potent but selective cytotoxicity are highly desirable. A novel series of triphenylstannyl 4-((arylimino)methyl)benzoates (**2-8**) were obtained by reactions of triphenylstannyl 4-formylbenzoate [$\text{Ph}_3\text{Sn}(\text{L}^1)$] **1** with primary aromatic amines. Two representative compounds (**10**, **11**) were also synthesized by reacting aqua-triphenylstannyl 2-formylbenzoate [$\text{Ph}_3\text{Sn}(\text{L}^9)(\text{H}_2\text{O})$] (**9**) with aniline and *p*-fluoroaniline, respectively. These compounds were characterized by elemental analysis, IR and ^1H , ^{13}C and ^{119}Sn NMR spectroscopies, as well as single-crystal X-ray diffraction for compounds **5**, **7-11** and three pro-ligands. In vitro cytotoxic activities of **1-11** were assessed by MMT tetrazolium dye assay against HeLa (human cervical) and MDA-MB-231 (breast) cancer cells; with IC_{50} values revealing high activity. Compared to cisplatin, compounds **1-11** exhibited enhanced cytotoxic efficacy, indicating their potential as potent anticancer agents. Among these, **1** and **5** demonstrated maximum inhibition in HeLa cells, with negligible effect on normal human embryonic kidney (HEK) cells. Combined results of DCFH-DA dye and Hoechst 33342/PI nuclear staining assays, along with flow cytometry analysis, show they possess a dual mode of action; induced apoptotic cell death, attributable to tin-assisted generation of reactive oxygen species. Cell cycle analyses indicated that compounds **1** and **5** exhibit cell growth inhibition and may cause turbulences in G1 and G2/M phases.

^aCentre for Advanced Studies in Chemistry, North-Eastern Hill University, NEHU Permanent Campus, Umshing, Shillong 793 022, India; E-mail: basubaul@nehu.ac.in, basubaulchem@gmail.com; Fax: +91-3642721000; Tel: +91-3642722626

^bSchool of Life & Environmental Science, Deakin University, Geelong, Victoria 3217, Australia

^cGenotoxicology and Cancer Biology Lab, Department of Zoology, Banaras Hindu University, Varanasi, India

^dCentro de Química Estrutural, Instituto Superior Técnico, Universidade de Lisboa, Av. Rovisco Pais 1, 1049-001 Lisboa, Portugal

†Electronic supplementary information (ESI) available: CCDC reference numbers 1533444-1533452. For ESI and crystallographic data in CIF format see DOI: XXXXX

Introduction

The extensive usage of cisplatin, *cis*-diamminedichloroplatinum(II) (CDDP) and analogous drugs is limited by drug resistance and severe side effects including neurotoxicity, gastrointestinal toxicity, and nephrotoxicity.¹⁻³ The first two are the major driving force behind current investigations and it is therefore of great significance to develop other metal based cancer chemotherapies. The substantial current investigation of other metal complexes (of Ru, Cu, Au, Pd, Fe, Co, Ti, Ga, Ni, Rh, Ir, Sn, Os, Zn, V, Ag, Re, Mo and lanthanide) is underway that may help to avoid or improve the problems associated with the use of platinum compounds.^{4,5} The chemistry of organotin(IV) compounds is one of the well-studied areas in organometallic chemistry and have shown acceptable in vitro cytotoxicity and antiproliferative in vivo activity as new chemotherapy agents besides diverse medicinal applications such as anti-viral, anti-microbial, anti-parasitic, anti-hypertensive, anti-hyperbilirubinemia activities.⁶⁻¹¹ Other sustainable chemistry applications include wood preservation to organic syntheses,¹² carbon dioxide capture,¹³ homogenous catalysts in PVC stabilisation, polyurethane formation and trans esterification.¹⁴ In the cancer chemotherapy arena, organotin(IV) compounds offer attractive properties such as not developing tumor drug tolerance, lower general toxicity than platinum drugs, fewer side effects, and no emetogenesis, better body clearance and increased water solubility.¹⁵ The current scenario in organotin chemistry is to attain an ideal point between the activity and toxicity of the compounds for their novel uses as antitumor agents. For this purpose, several triphenyltin(IV) carboxylates were investigated because the carboxylate group in the molecule is vital for aqueous solubility, which results in increased cellular accumulation,^{16,17} while the incorporation of the triphenyltin(IV) moiety in the molecule offers much higher activities when compared with titanocene derivatives and *cis*platin.¹⁸⁻²⁰ In this pursuit, a biocompatible strategy of drug delivery employing nanostructured silica-based material loaded with a triphenyltin(IV) compound has been used, resulting in an increase in efficacy of the drug.²¹ However, the design of organotin-based compounds with good therapeutic index is still rather empirical. Details of specific or selective bonding of organotin(IV) moiety to donor sites in biological structures is very limited and consequently reliable mechanisms of biological activity and valid structure-activity relationships are also limited. In previous studies, we have

shown how triphenyltin(IV) carboxylates of the appropriate diazo- and its isoelectronic imino- scaffolds were endowed with anticancer properties when the carboxylate functionality was varied between *ortho*-, *meta*- and *para*-positions.²²

On the other hand, Schiff bases are versatile ligands that have been utilized in modern organometallic and bioorganometallic chemistry.²³⁻²⁵ Schiff bases exhibit π -acceptor properties owing to the basic nature of the imine nitrogen atom and the presence of proximate donor groups influences the chelating ability, with the metal complexes used as catalysts in various reactions.²⁶⁻²⁸ The reversible nature of imine bonds provides access to dynamic covalent chemistry, which is employed for the creation of metal-organic materials, covalent organic frameworks, and self-assembled architectures that are promising for sustainable energy, environmental, and biological applications.²⁹⁻³⁹

At this juncture, it was thought worthwhile to combine the anticancer properties exhibited by the organotin(IV) compounds with the established biological effects of Schiff bases. The primary objective of this work was the synthesis and characterization of a large group of new organotin(IV) Schiff base derivatives where triphenyltin(IV) compounds are the focus of cytotoxicity studies. The choice of the triphenyltin(IV) derivatives was based upon previously established optimal balance between the cytotoxicity, solubility, and lipophilicity.²² With this precedent, in the current work the carboxylated Schiff base ligands were combined with the biologically and pharmacologically active triphenyltin moiety in a single chemical entity. It is believed that phenyltin(IV) derivatives may demonstrate efficacy with less toxicity than other organotin(IV) derivatives due to their interaction with the cell membrane.⁴⁰ Thus, it may be anticipated that combined effects of the resulting coordination compounds may improve the activity and this strategy perhaps could produce enhanced efficacy and reduced toxic effects.⁴¹ In an effort to improve the cytotoxic potential of the compounds, we investigated triphenylstannyl 4-formylbenzoate [$\text{Ph}_3\text{Sn}(\text{L}^1)$] (**1**) and its reaction products with primary aromatic amine condensates i.e. triphenylstannyl 4-((arylimino)methyl)benzoates (**2-8**), where the aniline R-group moiety was varied and the benzoic acid part of the molecule held constant. Additionally, two *ortho*-analogues i.e. triphenylstannyl 2-((arylimino)methyl)benzoates (**10-11**) were also isolated from the reactions of aqua-triphenylstannyl 2-

formylbenzoate $[\text{Ph}_3\text{Sn}(\text{L}^9)(\text{H}_2\text{O})]$ (**9**) with aniline and *p*-fluoroaniline, respectively (Scheme 1). These two derivatives are also reported here because modification of the carboxylate ligands can optimize cytotoxicity²² while varying the location of the triphenyltin ester can modulate the activity at a specific target. The pro-ligands HL^n ($n = 2-8$) and the triphenyltin complexed Schiff bases (**2-8**, **10** and **11**) were spectroscopically characterized and the crystal structures of representative compounds **5**, **7-11**, along with three pro-ligands HL^3 , HL^5 and HL^6 , were determined by single-crystal X-ray diffraction.

In preceding studies, we have shown how $[\text{Ph}_3\text{Sn}(\text{L}^n)]$ compounds (L^n is isomeric 2/3/4- $\{(E)-2-[4-(\text{dimethylamino})\text{phenyl}]\text{diazenyl}\}$ benzoates and their corresponding isoelectronic imino analogues 2/3/4- $\{(E)-\{[4-(\text{dimethylamino})\text{phenyl}]\text{methylidene}\}\text{amino}\}$ benzoates) were endowed with anticancer properties.²² Among these, triphenyltin(IV)-2- $\{(E)-2-[4-(\text{dimethylamino})\text{phenyl}]\text{diazenyl}\}$ benzoate and triphenyltin(IV)-4- $\{(E)-2-[4-(\text{dimethylamino})\text{phenyl}]\text{diazenyl}\}$ benzoate, both functionalized with a diazo group, displayed comparable activity towards MDA-MB-231 (human breast cancer) cells. On the other hand, triphenyltin(IV)-3- $\{(E)-\{[4-(\text{dimethylamino})\text{phenyl}]\text{methylidene}\}\text{amino}\}$ benzoate containing an imino framework demonstrated superior activity (31-folds compared to CDDP) towards HeLa (human cervical cancer) cells, importantly without affecting normal cells. The underlying investigation suggested that the compounds exert potent antitumor effect by elevating intracellular ROS (reactive oxygen species) generation and induce delay in cell cycle by inhibiting cells at G₂/M phase. In accordance with this and with the intention of selecting the best performing compounds for subsequent studies from a larger pool, the cytotoxic potential of the pro-ligands HL^n , 3-(phenylamino)isobenzofuran-1(3H)-one (Phthalide-H), 3-((4-fluorophenyl)amino)isobenzofuran-1(3H)-one (Phthalide-F), triphenyltin(IV) compounds **2-8**, **10** and **11**, as well as the two triphenyltin(IV) precursors **1** and **9**, were probed on the HeLa and MDA-MB-231 cells and to find a link between the structural modifications and the cytotoxic performances. In this work, we aimed to investigate whether triphenyltin compounds can induce intracellular oxidative stress and play a role in delaying cell cycle. This was probed using MTT (3-(4,5-dimethylthiazol-2-yl)-2,5-diphenyltetrazolium bromide) assay, DCFH-DA (dichlorodihydro-fluorescein diacetate) dye, Hoechst 33342/PI (propidium iodide), and PI staining studies.

Experimental

Materials and physical measurements.

Aniline (Sd Fine) was freshly distilled prior to use, while all other chemicals were used as purchased without purification: 4-formylbenzoic acid (**HL**¹), 2-formylbenzoic acid (**HL**⁹), triphenyltin hydroxide (Sigma Aldrich), *p*-toluidine (Merck), *p*-ethylamine (Sd Fine), *p*-anisidine (Sisco), *p*-ethoxyaniline, *p*-fluoroaniline (Spectrochem) and *N,N*-dimethyl-4-phenylenediamine (Alfa Aesar). Solvents were purified by standard procedures and were freshly distilled prior to use. Dulbecco's modified eagle medium (DMEM), fetal bovine serum (FBS) (Gibco, Life technologies), penicillin 1000 IU, streptomycin 10 mg/mL, *L*-glutamine, trypsin, EDTA (Genetix Biotech Asia) 3-(4,5-dimethylthiazol-2-yl)-2,5-diphenyltetrazoliumbromide dye (MTT) (Himedia), dimethyl sulphoxide (DMSO), RNase (GeNie, Merck), 2',7'-dichlorodihydrofluorescein diacetate (DCFH-DA), Hoechst 33342 (Sigma), propidium iodide (PI) (EMD Millipore-Calbiochem), cytoplatin (Cipla; generic name- cisplatin), Triton X-100 and other analytical grade chemicals (Lobachemie) were used. Melting points were measured using a Büchi melting point apparatus M-560 and are uncorrected. Elemental analyses were performed using a Perkin Elmer 2400 series II instrument. IR spectra in the range 4000-400 cm⁻¹ were obtained on a Perkin Elmer Spectrum BX series FT-IR spectrophotometer with samples investigated as KBr discs. ¹H and ¹³C NMR spectra of pro-ligands and triphenyltin(IV) compounds (**1-11**) were recorded on a Bruker AMX 400 spectrometer and measured at 400.13 and 100.62 MHz, respectively. ¹¹⁹Sn NMR spectra were measured on a Jeol GX 270 spectrometer at 100.75 MHz. The ¹H, ¹³C and ¹¹⁹Sn chemical shifts were referenced to Me₄Si (δ 0.00 ppm), CDCl₃ (δ 77.00 ppm), and Me₄Sn (δ 0.00 ppm), respectively. Equipment such as ELISA plate reader microscan (ECIL, Hyderabad, MS 5608A), inverted fluorescence microscopy (Nikkon E800) and inverted fluorescent microscope (Evos FL, Life technologies, AMF4300) were used for biological work.

Synthesis of pro-ligands

Synthesis of (*E*)-4-((phenylimino)methyl)benzoic acid (HL**²).** A toluene solution (2 mL) of aniline (0.15 g, 1.611 mmol) was added to a hot toluene solution (50 mL) containing 4-formylbenzoic acid (0.25 g,

1.665 mmol). The reaction mixture was heated to reflux for 4 h using a Dean-Stark apparatus, whereupon the solution turned yellow. It was filtered while hot and the filtrate concentrated to one third of its initial solvent volume, which upon standing at room temperature deposited a yellow microcrystalline product. The residue was boiled with hexane (3 x 5 mL), filtered and dried *in vacuo*. The crude product was then recrystallized from acetonitrile to give a yellow crystalline material in 51 % (0.21 g) yield. M.p.: 228-230 °C. Anal. Found. C, 74.50; H, 5.10; N, 6.28. Calc. for C₁₄H₁₁NO₂: C, 74.65; H, 4.92; N, 6.22 %. IR (cm⁻¹): 1679 ν(OCO)_{asym}, 1621 ν(C(H)=N), 1424, 1318, 1287, 1193, 775, 763, 699. ¹H NMR (DMSO-*d*₆): δ_H; 8.70 [s, 1H, H-6], 7.57-8.15 [m, 4H, H-3 and H-4], 7.35-7.5 [m, 2H, H-8], 7.20-7.35 [m, 3H, H-9 and H-10] ppm. ¹³C NMR (DMSO-*d*₆): δ_C; 166.9 [C-1], 159.8 [C-6], 150.9, 139.5, 132.9, 129.7, 129.2, 128.7, 126.4, 121.1, 115.6, 113.8 [Ar-C] ppm.

Synthesis of (*E*)-4-((*p*-tolylimino)methyl)benzoic acid (HL³). An analogous method to that used for the preparation of HL² was followed except that aniline was replaced by *p*-toluidine (0.18 g, 1.682 mmol). The product was crystallized from acetonitrile-DMF (10:1 v/v) mixture, giving yellow crystals of HL³ in 63% yield. M.p.: 260-262 °C. Anal. Found. C, 74.90; H, 5.10; N, 6.28. Calc. for C₁₅H₁₃NO₂: C, 75.30; H, 5.48; N, 5.85 %. IR (cm⁻¹): 1685 ν(OCO)_{asym}, 1624 ν(C(H)=N), 1501, 1423, 1309, 1288, 1125, 858, 539. ¹H NMR (DMSO-*d*₆): δ_H; 8.48 [s, 1H, H-6], 7.75-7.90 [m, 4H, H-3 and H-4], 6.95-7.08 [m, 4H, H-8 and H-9], 2.09 [s, 3H, H-11] ppm. ¹³C NMR (DMSO-*d*₆): δ_C; 166.9 [C-1], 158.7 [C-6], 148.3, 139.7, 135.9, 132.9, 129.7, 129.6, 128.5, 121.1 [Ar-C], 20.6 [C-11] ppm.

Synthesis of (*E*)-4-(((*p*-ethylphenyl)imino)methyl)benzoic acid (HL⁴). An analogous method to that used for the preparation of HL² was followed except that aniline was replaced by *p*-ethylaniline (0.17 g, 1.665 mmol). The product was crystallized from acetonitrile, giving yellow crystals of HL⁴ in 82% yield. M.p.: 240-242 °C. Anal. Found. C, 76.10; H, 5.90; N, 5.29. Calc. for C₁₆H₁₅NO₂: C, 75.87; H, 5.97; N, 5.53 %. IR (cm⁻¹): 1683 ν(OCO)_{asym}, 1625ν(C(H)=N), 1610, 1499, 1426, 1319, 1291, 944, 553. ¹H NMR (DMSO-*d*₆): δ_H; 8.49 [s, 1H, H-6], 7.75-7.90 [m, 4H, H-3 and H-4], 6.95-7.10 [m, 4H, H-8 and H-9], 2.39 and 0.96

[q, 7Hz, 2H and t, 6 Hz, 3H, H-11] ppm. ^{13}C NMR (DMSO- d_6): δ_{C} ; 166.9 [C-1], 158.8 [C-6], 148.5, 142.3, 139.7, 132.8, 129.6, 128.5, 121.1, 113.9 [Ar-C], 27.7 and 15.6 [C-11] ppm.

Synthesis of (*E*)-4-(((*p*-methoxyphenyl)imino)methyl)benzoic acid (HL**⁵).** An analogous method to that used for the preparation of **HL**² was followed except that aniline was replaced by *p*-anisidine (0.21 g, 1.705 mmol). The product was crystallized from methanol, giving yellow crystals of **HL**⁵ in 68% yield. M.p.: 224-226 °C. Anal. Found. C, 70.44; H, 5.20; N, 5.22. Calc. for C₁₅H₁₃NO₃: C, 70.58; H, 5.13; N, 5.49 %. IR (cm⁻¹): 1686 $\nu(\text{OCO})_{\text{asym}}$, 1621 $\nu(\text{C(H)=N})$, 1501, 1429, 1364, 1310, 1287, 1247, 1030, 835, 791, 549. ^1H NMR (DMSO- d_6): δ_{H} ; 8.78 [s, 1H, H-6], 8.00-8.20 [m, 4H, H-3 and H-4], 7.41 [d, 8 Hz, 2H, H-8], 7.05 [d, 8 Hz, 2H, H-9], 3.84 [s, 3H, H-11] ppm. ^{13}C NMR (DMSO- d_6): δ_{C} ; 166.9 [C-1], 158.3 [C-6], 157.2, 143.5, 139.9, 132.5, 129.6, 128.3, 122.6, 114.4 [Ar-C], 55.2 [C-11] ppm.

Synthesis of (*E*)-4-(((*p*-ethoxyphenyl)imino)methyl)benzoic acid (HL**⁶).** An analogous method to that used for the preparation of **HL**² was followed except that aniline was replaced by *p*-ethoxyaniline (0.23 g, 1.677 mmol). The product was crystallized from acetonitrile-DMF (10:1 v/v) mixture, giving yellow crystals of **HL**⁶ in 80% yield. M.p.: 237-239 °C. Anal. Found. C, 70.94; H, 5.28; N, 5.22. Calc. for C₁₆H₁₅NO₃: C, 71.36; H, 5.61; N, 5.20 %. IR (cm⁻¹): 1678 $\nu(\text{OCO})_{\text{asym}}$, 1625 $\nu(\text{C(H)=N})$, 1591, 1503, 1424, 1288, 1245, 1116, 1046, 797, 541. ^1H NMR (DMSO- d_6): δ_{H} ; 8.71 [s, 1H, H-6], 7.90-8.10 [m, 4H, H-3 and H-4], 7.32 [d, 8 Hz, 2H, H-8], 6.96 [d, 8 Hz, 2H, H-9], 4.02 and 1.31 [q, 7Hz, 2H and t, 6Hz, 3H, H-11] ppm. ^{13}C NMR (DMSO- d_6): δ_{C} ; 166.9 [C-1], 157.6, 157.1 [C-6], 143.4, 139.9, 132.5, 129.6, 128.3, 122.6, 114.8 [Ar-C], 63.2 and 14.6 [C-11] ppm.

Synthesis of (*E*)-4-(((*p*-fluorophenyl)imino)methyl)benzoic acid (HL**⁷).** An analogous method to that used for the preparation of **HL**² was followed except that aniline was replaced by *p*-fluoroaniline (0.18 g, 1.665 mmol). The product was crystallized from ethanol, giving yellow crystals of **HL**⁷ in 59% yield. M.p.: 232-234 °C. Anal. Found. C, 69.40; H, 4.28; N, 6.12. Calc. for C₁₄H₁₀FNO₃: C, 69.13; H, 4.14; N, 5.76 %.

IR (cm^{-1}): 1680 $\nu(\text{OCO})_{\text{asym}}$, 1622 $\nu(\text{C(H)=N})$, 1568, 1500, 1424, 1369, 1289, 1218, 1189, 1126, 860, 836, 801, 774, 538. ^1H NMR ($\text{DMSO-}d_6$): δ_{H} ; 8.78 [s, 1H, H-6], 8.0-8.20 [m, 4H, H-3 and H-4], 7.40 [m, 2H, H-8], 7.25-7.50 [m, 2H, H-9] ppm. ^{13}C NMR ($\text{DMSO-}d_6$): δ_{C} ; 166.8 [C-1], 162.0, 159.8 [C-6], 159.6, 147.2, 139.5, 132.9, 129.7, 128.6, 123.0 and 122.9, 116.0 and 115.8 [Ar-C] ppm.

Synthesis of (E)-4-(((p-(dimethylamino)phenyl)imino)methyl)benzoic acid (HL^8). An analogous method to that used for the preparation of HL^2 was followed except that aniline was replaced by N,N-dimethyl-p-phenylenediamine (0.20 g, 1.644 mmol). The product was crystallized from acetonitrile, giving dark yellow crystals of HL^8 in 67% yield. M.p.: 265-267 °C (dec.). Anal. Found. C, 71.40; H, 6.28; N, 10.42. Calc. for $\text{C}_{16}\text{H}_{16}\text{N}_2\text{O}_2$: C, 71.62; H, 6.01; N, 10.44 %. IR (cm^{-1}): 1683 $\nu(\text{OCO})_{\text{asym}}$, 1621 $\nu(\text{C(H)=N})$, 1586, 1514, 1420, 1358, 1282, 1123, 944, 820, 603. ^1H NMR ($\text{DMSO-}d_6$): δ_{H} ; 8.64 [s, 1H, H-6], 7.85-8.00 [m, 4H, H-3 and H-4], 7.25 [d, 8 Hz, 2H, H-8], 6.68 [d, 8 Hz, 2H, H-9], 2.86 [s, 3H, H-11] ppm. ^{13}C NMR ($\text{DMSO-}d_6$): δ_{C} ; 167.0 [C-1], 153.6 [C-6], 149.7, 140.4, 139.0, 131.9, 129.6, 127.9, 122.7, 112.4 [Ar-C], 40.1 [C-11] ppm.

Note: Synthesis of (E)-2-((phenylimino)methyl)benzoic acid and (E)-2-(((4-fluorophenyl)imino)methyl)benzoic acid could not be accomplished since equimolar reactions of aniline and p-fluoroaniline with 2-formylbenzoic acid in refluxing toluene proceeded via cyclization to give 3-(phenylamino)isobenzofuran-1(3H)-one (Phthalide-H) and 3-((4-fluorophenyl)amino)isobenzofuran-1(3H)-one (Phthalide-F), respectively. Phthalide-H was isolated as colorless crystals from acetonitrile in 77% yield, M.p.: 182-183 °C (180-181°C when crystallized from aqueous acetone,⁴² 179-180°C when crystallized from dimethylformamide.⁴³). IR (cm^{-1}): 1740 $\nu(\text{OCO})$ lactonic moiety, 1606, 1529, 1500, 1358, 1305, 1262, 1208, 1099, 1080, 871, 744, 693, 503. Formation of the products was also confirmed from the ^1H NMR and single crystal X-ray diffraction.⁴³ Phthalide-F was isolated as colorless crystals from acetonitrile in 75% yield, M.p.: 189-191 °C. IR (cm^{-1}): 1736 $\nu(\text{OCO})$ lactonic moiety, 1611, 1528, 1511, 1308, 1230, 1159, 1093, 870, 824, 787, 747, 512. ^1H NMR ($\text{DMSO-}d_6$): δ_{H} ; 7.80-7.92 [m, 2H, ArH], 7.65-

7.75 [m, 2H, ArH], 7.0-7.18 [m, 3H, ArH], 6.85-7.0 [m, 2H, ArH] ppm. ^{13}C NMR (DMSO- d_6): δ_{C} : 168.8, 157.5, 155.1, 145.4, 141.2, 133.8, 130.1, 127.5, 124.5, 123.7, 115.3, 115.1, 88.2 [Ar-C] ppm.

Synthesis of triphenyltin(IV) compounds 1-11

The triphenyltin(IV) compounds reported here are numbered as **1-11** (see Scheme 1) for convenience of discussion. Details of the procedures have been outlined below.

Synthesis of [Ph₃Sn(L¹)] (1). Ph₃SnOH (0.2 g, 0.545 mmol) in toluene (20 mL) was added to a hot toluene solution (20 mL) containing 4-formylbenzoic acid (0.08 g, 0.533 mmol). The reaction mixture was heated to reflux for 4 h using a Dean-Stark apparatus and water-cooled condenser, then filtered while hot and the filtrate evaporated to dryness. The dry residue was washed with hexane (3 × 5 mL) and dried *in vacuo*. The residue was dissolved in the minimum amount of anhydrous benzene and filtered to remove any suspended particles. The filtrate was concentrated to approximately one-fourth of its initial solvent volume, cooled to room temperature, precipitated with hexane, filtered and the residue was dried *in vacuo*. The dried powder was recrystallized from benzene, which afforded white crystalline material of **1**. Yield: 40 %. M.p.: 155-157 °C. Anal. Found. C, 62.40; H, 4.28. Calc. for C₂₆H₂₀O₃Sn: C, 62.56; H, 4.04 %. IR (cm⁻¹): 1661 $\nu(\text{OCO})_{\text{asym}}$, 1572, 1429, 1330, 1317, 1213, 1128, 816, 765, 732, 696, 584. ^1H NMR (CDCl₃): δ_{H} ; 10.1 [s, 1H, H-6], 8.28 [d, 8 Hz, 2H, H-4], 7.91 [d, 8 Hz, 2H, H-3], 7.75-7.84 [m, 6H, H-2* (Sn-Ph)], 7.40-7.51 [m, 9H, H-3* and H4* (Sn-Ph)] ppm. ^{13}C NMR (CDCl₃): δ_{C} ; 191.9 [C-6], 171.5 [C-1], 138.9 [C-5], 136.0 [C-2], 131.2 [C-3], 129.5 [C-4]; Sn-Ph: 137.9 [$^1J(^{13}\text{C}-^{119}\text{Sn}) = 643$ Hz, C-1*], 137.0 [$^2J(^{13}\text{C}-^{119}\text{Sn}) = 48$ Hz, C-2*], 130.4 [$^4J(^{13}\text{C}-^{119}\text{Sn}) = 13$ Hz, C-4*], 129.1 [$^3J(^{13}\text{C}-^{119}\text{Sn}) = 62$ Hz, C-3*] ppm. ^{119}Sn NMR (CDCl₃): δ_{Sn} : -99.8 ppm. (Note: 1*, 2*, 3* and 4* refer to *ipso*-, *ortho*-, *meta*- and *para*- carbon and proton numbers of Sn-Ph moiety used for the assignment of NMR signals and applies to all triphenyltin(IV) compounds).

Synthesis of [Ph₃Sn(L²)] (2). A toluene solution (2 mL) of aniline (0.046 g, 0.490 mmol) was added to a hot clear toluene solution (40 mL) containing **1** (0.25 g, 0.500 mmol) and then heated to reflux for 4 h

using a Dean-Stark apparatus, whereupon the solution turned pale yellow. The reaction mixture was filtered while hot and the filtrate concentrated to dryness, affording a viscous mass that was stored *in vacuo* overnight. The solid material was dissolved by boiling in benzene and filtered to remove any suspended particles. The filtrate was concentrated to one-fourth of its initial volume and precipitated with hexane, affording the crude product. Several crystallizations using benzene/hexane mixture afforded a pale yellow crystalline material in 57 % (0.17 g) yield. M.p.: 158-160 °C. Anal. Found. C, 67.10; H, 4.60; N, 2.28. Calc. for C₃₂H₂₅NO₂Sn: C, 66.93; H, 4.39; N, 2.44 %. IR (cm⁻¹): 1635 ν(OCO)_{asym}, 1619 ν(C(H)=N), 1481, 1338, 1127, 730, 695. ¹H NMR (CDCl₃): δ_H; 8.70 [s, 1H, H-6], 8.16 [d, 8.0 Hz, 2H, H-3], 7.86 [d, 2H, H-4], 7.70-7.80 [m, 6H, H-2* (Sn-Ph)], 7.25-7.50 [m, 11H, H-3*, H-4* and H-8], 7.10-7.25 [m, 3H, H-9 and H-10] ppm. ¹³C NMR (CDCl₃): δ_C; 172.1 [C-1], 159.4 [C-6], 151.6, 138.1, 133.0, 131.2, 131.0, 129.2, 128.5, 126.4 [Ar-C], Sn-Ph: 139.7 [¹J(¹³C-¹¹⁹Sn) = 640 Hz, C-1*], 137.0 [²J(¹³C-¹¹⁹Sn) = 48 Hz, C-2*], 130.3 [⁴J(¹³C-¹¹⁹Sn) = 13 Hz, C-4*], 129.0 [³J(¹³C-¹¹⁹Sn) = 62 Hz, C-3*] ppm. ¹¹⁹Sn NMR (CDCl₃); δ_{Sn}: -104.9 ppm.

Synthesis of [Ph₃Sn(L³)] (3). An analogous method to that used for the preparation of **2** was followed using **1** and *p*-toluidine (0.05 g, 0.478 mmol). The product was crystallized from *n*-heptane, giving yellow crystals of compound **3** in 40% yield. M.p.: 150-152 °C. M.p.: 150-152 °C. Anal. Found. C, 67.60; H, 4.80; N, 2.08. Calc. for C₃₃H₂₇NO₂Sn: C, 67.37; H, 4.63; N, 2.38 %. IR (cm⁻¹): 1625 ν(OCO)_{asym} + ν(C(H)=N), 1539, 1430, 1341, 1128, 814, 731, 697. ¹H NMR (CDCl₃): δ_H; 8.40 [s, 1H, H-6], 8.11 [d, 8 Hz, 2H, H-3], 7.84 [d, 8 Hz, 2H, H-4], 7.65-7.75 [m, 6H, H-2* (Sn-Ph)], 7.25-7.45 [m, 9H, H-3* and H-4*], 7.0-7.15 [m, 4H, H-8 and H-9], 2.72 [s, 3H, H-11] ppm. ¹³C NMR (CDCl₃): δ_C; 172.2 [C-1], 158.5 [C-6], 149.0, 138.2, 136.4, 132.8, 131.0, 129.9, 128.4, 120.9 [Ar-C], 21.1 [C-11], Sn-Ph: 139.9 [¹J(¹³C-¹¹⁹Sn) = 645 Hz, C-1*], 137.0 [²J(¹³C-¹¹⁹Sn) = 48 Hz, C-2*], 130.3 [⁴J(¹³C-¹¹⁹Sn) = 13 Hz, C-4*], 129.0 [³J(¹³C-¹¹⁹Sn) = 62 Hz, C-3*] ppm. ¹¹⁹Sn NMR (CDCl₃); δ_{Sn}: -105.2 ppm.

Synthesis of [Ph₃Sn(L⁴)] (4). An analogous method to that used for the preparation of **2** was followed using *p*-ethylalaniline (0.06 g, 0.495 mmol). The product was crystallized from benzene/hexane (3:1 v/v) mixture, giving bright yellow crystals of compound **4** in 41% yield. M.p.: 120-122 °C. Anal. Found. C, 67.98; H, 4.95; N, 2.11. Calc. for C₃₄H₂₉NO₂Sn: C, 67.80; H, 4.85; N, 2.33 %. IR (cm⁻¹): 1624 ν(OCO)_{asym} + ν(C(H)=N), 1345, 1128, 1077, 777, 729, 697. ¹H NMR (CDCl₃): δ_H; 8.44 [s, 1H, H-6], 8.15 [d, 8 Hz, 2H, H-3], 7.87 [d, 8 Hz, 2H, H-4], 7.70-7.80 [m, 6H, H-2* (Sn-Ph)], 7.35-7.50 [m, 9H, H-3* and H-4* (Sn-Ph)], 7.05-7.20 [m, 4H, H-8 and H-9], 2.60 and 1.18 [q, 7 Hz, 2H and t, 6 Hz, 3H, H-11] ppm. ¹³C NMR (CDCl₃): δ_C; 172.8 [C-1], 158.5 [C-6], 149.1, 142.8, 138.1, 131.2, 131.0, 129.3, 128.7, 128.4, 121.0 [Ar-C], 28.5 and 15.7 [C-11], Sn-Ph: 140.0 [¹J(¹³C-¹¹⁹Sn) = 640 Hz, C-1*], 136.9 [²J(¹³C-¹¹⁹Sn) = 48 Hz, C-2*], 130.3 [⁴J(¹³C-¹¹⁹Sn) = 13 Hz, C-4*], 129.0 [³J(¹³C-¹¹⁹Sn) = 62 Hz, C-3*] ppm. ¹¹⁹Sn NMR (CDCl₃): δ_{Sn}: -105.3 ppm.

Synthesis of [Ph₃Sn(L⁵)] (5). An analogous method to that used for the preparation of **2** was followed using *p*-anisidine (0.07 g, 0.557 mmol). The product was crystallized from acetonitrile, giving yellow crystals of compound **5** in 56% yield. M.p.: 160-162 °C. Anal. Found. C, 67.08; H, 4.85; N, 2.05. Calc. for C₃₃H₂₇NO₃Sn: C, 66.59; H, 4.50; N, 2.32 %. IR (cm⁻¹): 1629 ν(OCO)_{asym} + ν(C(H)=N), 1501, 1430, 1340, 1250, 1128, 1035, 829, 736, 697. ¹H NMR (CDCl₃): δ_H; 8.43 [s, 1H, CH=N], 8.13 [d, 8 Hz, 2H, H-3], 7.84 [d, 8 Hz, 2H, H-4], 7.70-7.80 [m, 6H, H-2* (Sn-Ph)], 7.35-7.50 [m, 9H, H-3* and H-4* (Sn-Ph)], 7.18 [d, 8 Hz, 2H, H-8], 6.85 [d, 8 Hz, 2H, H-9], 3.75 [s, 3H, H-11] ppm. ¹³C NMR (CDCl₃): δ_C; 172.3 [C-1], 158.7, 157.1 [C-6], 144.4, 138.2, 132.6, 131.0, 128.3, 122.4, 114.4 [Ar-C], 55.5 [C-11]; Sn-Ph: 140.1 [¹J(¹³C-¹¹⁹Sn) = 640 Hz, C-1*], 137.0 [²J(¹³C-¹¹⁹Sn) = 48 Hz, C-2*], 130.3 [⁴J(¹³C-¹¹⁹Sn) = 13 Hz, C-4*], 129.0 [³J(¹³C-¹¹⁹Sn) = 62 Hz, C-3*] ppm. ¹¹⁹Sn NMR (CDCl₃): δ_{Sn}: -105.6 ppm.

Synthesis of [Ph₃Sn(L⁶)]·C₆H₆ (6). An analogous method to that used for the preparation of **2** was followed using *p*-ethoxyaniline (0.08 g, 0.572 mmol). The product was crystallized from methanol/benzene

(3:1 v/v) mixture, giving bright yellow crystals of compound **6** in 66% yield. M.p.: 136-138 °C. Anal. Found. C, 68.50; H, 4.75; N, 2.45. Calc. for C₄₀H₃₅NO₃Sn: C, 68.97; H, 5.07; N, 2.01 %. IR (cm⁻¹): 1628 $\nu(\text{OCO})_{\text{asym}}$, 1590 $\nu(\text{C(H)=N})$, 1503, 1430, 1338, 1285, 1251, 1126, 827, 731, 698. ¹H NMR (CDCl₃): 8.04 [s, 1H, CH=N], 8.11 [d, 8 Hz, 2H, H-3], 7.81 [d, 8 Hz, 2H, H-4], 7.65-7.75 [m, 6H, H-2* (Sn-Ph)], 7.30-7.40 [m, 9H, H-3* and H-4* (Sn-Ph)], 7.15 [d, 8 Hz, 2H, H-8], 6.81 [d, 8 Hz, 2H, H-9], 3.93 and 1.30 [q, 7Hz, 2H and t, 6 Hz, 3H, H-11] ppm. ¹³C NMR (CDCl₃): δ_{C} ; 172.2 [C-1], 158.1, 157.0 [C-6], 144.2, 138.1, 132.5, 131.0, 128.3, 122.4, 114.9 [Ar-C], 63.7 and 14.9 [C-11], Sn-Ph: 140.1 [¹J(¹³C-¹¹⁹Sn) = 640 Hz, C-1*], 137.0 [²J(¹³C-¹¹⁹Sn) = 48 Hz, C-2*], 130.3 [⁴J(¹³C-¹¹⁹Sn) = 13 Hz, C-4*], 129.0 [³J(¹³C-¹¹⁹Sn) = 62 Hz, C-3*] ppm. ¹¹⁹Sn NMR (CDCl₃); δ_{Sn} : -105.7 ppm.

Synthesis of [Ph₃Sn(L⁷)] (7). An analogous method to that used for the preparation of **2** was followed using *p*-fluoroaniline (0.06 g, 0.540 mmol). The product was crystallized from acetonitrile/methanol (3:1 v/v) mixture, giving yellow crystals of compound **7** in 57% yield. M.p.: 171-173 °C. Anal. Found. C, 65.12; H, 4.45; N, 2.25. Calc. for C₃₂H₂₄FNO₂Sn: C, 64.90; H, 4.08; N, 2.37 %. IR (cm⁻¹): 1634 $\nu(\text{OCO})_{\text{asym}}$, 1623 $\nu(\text{C(H)=N})$, 1499, 1330, 1300, 832, 730, 695. ¹H NMR (CDCl₃): 8.41 [s, 1H, CH=N], 8.16 [d, 8 Hz, 2H, H-3], 7.86 [d, 8 Hz, 2H, H-4], 7.70-7.80 [m, 6H, H-2* (Sn-Ph)], 7.35-7.50 [m, 9H, H-3* and H-4* (Sn-Ph)], 7.10-7.20 [m, 2H, H-8], 6.95-7.10 [m, 2H, H-9] ppm. ¹³C NMR (CDCl₃): δ_{C} ; 171.4 [C-1], 162.7, 160.3, 159.1 [C-6], 147.7, 138.1, 131.2, 131.0, 128.5, 129.3, 128.5, 128.4, 122.5, 122.4, 116.1, 115.9 [Ar-C], Sn-Ph: 139.6 [¹J(¹³C-¹¹⁹Sn) = 640 Hz, C-1*], 137.0 [²J(¹³C-¹¹⁹Sn) = 48 Hz, C-2*], 130.3 [⁴J(¹³C-¹¹⁹Sn) = 13 Hz, C-4*], 129.0 [³J(¹³C-¹¹⁹Sn) = 62 Hz, C-3*] ppm. ¹¹⁹Sn NMR (CDCl₃); δ_{Sn} : -104.7 ppm.

Synthesis of [Ph₃Sn(L⁸)] (8). An analogous method to that used for the preparation of **2** was followed using *N,N*-dimethyl-*p*-phenylenediamine (0.06 g, 0.491 mmol). The product was crystallized from acetonitrile, giving bright yellow crystals of compound **8** in 63% yield. M.p.: 167-169 °C. Anal. Found. C,

65.83; H, 5.35; N, 4.75. Calc. for $C_{34}H_{30}N_2O_2Sn$: C, 66.15; H, 4.90; N, 4.54 %. IR (cm^{-1}): 1619 $\nu(OCO)_{asym}$, 1580 $\nu(C(H)=N)$, 1517, 1480, 1430, 1342, 1163, 1126, 857, 818, 777, 730, 696, 537. 1H NMR ($CDCl_3$): 8.47 [s, 1H, CH=N], 8.12 [d, 8 Hz, 2H, H-3], 7.83 [d, 8 Hz, 2H, H-4], 7.65-7.80 [m, 6H, H-2* (Sn-Ph)], 7.30-7.45 [m, 9H, H-3* and H-4* (Sn-Ph)], 7.22 [d, 8 Hz, 2H, H-8], 6.67 [d, 8 Hz, 2H, H-9], 2.91 [s, 3H, H-11] ppm. ^{13}C NMR ($CDCl_3$): δ_C : 172.3 [C-1], 154.3 [C-6], 149.9, 140.6, 138.2, 132.0, 131.0, 127.9, 122.6, 112.7, [Ar-C], 40.6 [C-11], Sn-Ph: 140.1 [$^1J(^{13}C-^{119}Sn) = 640$ Hz, C-1*], 137.0 [$^2J(^{13}C-^{119}Sn) = 48$ Hz, C-2*], 130.2 [$^4J(^{13}C-^{119}Sn) = 13$ Hz, C-4*], 129.0 [$^3J(^{13}C-^{119}Sn) = 62$ Hz, C-3*] ppm. ^{119}Sn NMR ($CDCl_3$); δ_{Sn} : -107.1 ppm.

Synthesis of $[Ph_3Sn(L^9)(H_2O)]$ (9). An analogous method to that used for the preparation of **1** was followed except that 4-formylbenzoic acid was replaced by 2-formylbenzoic acid. The product was crystallized from acetonitrile, giving colorless crystals of compound **9** in 91% yield. M.p.: 120-122 °C. Anal. Found. C, 60.98; H, 3.85. Calc. for $C_{26}H_{22}O_4Sn$: C, 60.36; H, 4.29 %. IR (cm^{-1}): 1663 $\nu(OCO)_{asym}$, 1636, 1589, 1389, 1341, 1262, 1109, 729, 697. 1H NMR ($CDCl_3$): 10.71 [s, 1H, H-8], 8.05 [br d, 1H, H-3], 7.65-7.90 [m, 7H, H-2* (Sn-Ph) and H-6], 7.50-7.60 [m, 2H, H-4 and H-5], 7.35-7.45 [m, 9H, H-3* and H-4* (Sn-Ph)] ppm. ^{13}C NMR ($CDCl_3$): δ_C : 193.1 [C-8], 172.2 [C-1], 137.5, 132.8, 132.2, 131.7, 127.9 [Ar-C], Sn-Ph: 137.8 [$^1J(^{13}C-^{119}Sn) = 640$ Hz, C-1*], 136.9 [$^2J(^{13}C-^{119}Sn) = 48$ Hz, C-2*], 130.5 [$^4J(^{13}C-^{119}Sn) = 13$ Hz, C-4*], 129.1 [$^3J(^{13}C-^{119}Sn) = 62$ Hz, C-3*] ppm. ^{119}Sn NMR ($CDCl_3$); δ_{Sn} : -98.3 ppm.

Synthesis of $[Ph_3Sn(L^{10})]$ (10). A toluene solution (2 mL) of aniline (0.046 g, 0.490 mmol) was added to a hot clear toluene solution (40 mL) containing **9** (0.25 g, 0.500 mmol) and then heated to reflux for 4 h using a Dean-Stark apparatus, whereupon the solution turned pale yellow. The reaction mixture was filtered while hot and the filtrate concentrated to dryness, affording a viscous mass that was triturated with ice-cold hexane (soluble in hexane) until free pale yellow powder was obtained. The solid was dissolved in hexane/benzene (3:1 v/v) mixture, filtered and allowed to evaporate slowly at room temperature, which

afforded bright yellow crystals of **10** in 58 % (0.17 g) yield. M.p.: 114-116 °C. Anal. Found. C, 66.90; H, 4.80; N, 2.50. Calc. for C₃₂H₂₅NO₂Sn: C, 66.93; H, 4.39; N, 2.44 %. IR (cm⁻¹): 1626 ν(OCO)_{asym}, 1610 ν(C(H)=N), 1480, 1431, 1340, 1189, 1142, 1076, 769, 731, 697. ¹H NMR (CDCl₃): 9.41 [s, 1H, H-8], 8.21 [br d, 2H, H-3 and H-6], 7.52-7.90 [m, 7H, H-2* (Sn-Ph) and H-6], 7.35-7.55 [m, 12H, H-3*, H4* (Sn-Ph), remaining ArH], 7.15-7.35 [m, 3H, H-11 and H-12] ppm. ¹³C NMR (CDCl₃): δ_C; 173.3 [C-1], 160.8 [C-8], 137.3, 132.3, 131.8, 131.3, 129.1, 128.1, 126.0, 121.3 [Ar-C], Sn-Ph: 138.1 [¹J(¹³C-¹¹⁹Sn) = 640 Hz, C-1*], 136.9 [²J(¹³C-¹¹⁹Sn) = 48 Hz, C-2*], 130.3 [⁴J(¹³C-¹¹⁹Sn) = 13 Hz, C-4*], 129.0 [³J(¹³C-¹¹⁹Sn) = 62 Hz, C-3*] ppm. ¹¹⁹Sn NMR (CDCl₃); δ_{Sn}: -103.7 ppm.

Synthesis of [Ph₃Sn(L¹¹)] (11**).** An analogous method to that used for the preparation of **10** was followed except that aniline was replaced by *p*-fluoroaniline (0.06 g, 0.540 mmol). The product was crystallized from hexane/benzene (3:1, v/v) mixture giving bright yellow crystals of compound **11** in 49% yield. M.p.: 89-91 °C. Anal. Found. C, 65.44; H, 4.88; N, 2.52. Calc. for C₃₂H₂₄FNO₂Sn: C, 64.90; H, 4.08; N, 2.37 %. IR (cm⁻¹): 1627 ν(OCO)_{asym}, 1590 ν(C(H)=N), 1501, 1480, 1430, 1350, 1232, 1185, 1080, 836, 733, 698. ¹H NMR (CDCl₃): 9.24 [s, 1H, H-8], 8.00-8.20 [m, 2H, H-3 and H-6], 7.51-7.53 [m, 6H, H-2* (Sn-Ph)], 7.35-7.55 [m, 11H, H-3*, H4* (Sn-Ph), H-4 and H-5], 7.00-7.10 [m, 2H, H-10], 6.90-7.00 [m, 2H, H-11] ppm. ¹³C NMR (CDCl₃): δ_C; 173.2 [C-1], 162.5, 160.5 [C-8], 160.1, 148.1, 132.2, 131.7, 131.3, 128.0, 122.8, 122.7, 115.9, 115.7 [Ar-C], Sn-Ph: 138.1 [¹J(¹³C-¹¹⁹Sn) = 640 Hz, C-1*], 136.9 [²J(¹³C-¹¹⁹Sn) = 48 Hz, C-2*], 130.3 [⁴J(¹³C-¹¹⁹Sn) = 13 Hz, C-4*], 129.0 [³J(¹³C-¹¹⁹Sn) = 62 Hz, C-3*] ppm. ¹¹⁹Sn NMR (CDCl₃); δ_{Sn}: -103.2 ppm.

X-ray crystallography

Crystals of compounds suitable for X-ray crystal-structure determination were obtained by slow evaporation of acetonitrile (**5**, **8** and **9**), acetonitrile/methanol (**7**), DMF/acetonitrile (**HL**³ and **HL**⁶), hexane (**10**), hexane/benzene (**11**) and methanol (**HL**⁵) solutions of the respective compounds at room temperature.

Diffraction data were recorded at ambient temperature on an Agilent Technologies Gemini area-detector diffractometer⁴⁴ using Mo K α radiation ($\lambda = 0.71073 \text{ \AA}$). The structures were solved by direct methods using the SIR-97 program⁴⁵ and refined with SHELXL-2014/7.⁴⁶ Calculations were performed using the WinGX System-Version 2014.1.⁴⁷ All non-hydrogen atoms were refined anisotropically. Hydrogen atoms bonded to carbon atoms were included in calculated positions and refined using the riding-model approximation with $U_{\text{iso}}(\text{H})$ defined as $1.2U_{\text{eq}}$ of the parent carbon atoms for phenyl and methyne residues and $1.5U_{\text{eq}}$ of the parent carbon atoms for the methyl group. Hydrogen atoms attached to oxygen have been located from the final difference Fourier map and their isotropic thermal parameter set as 1.5 times the average thermal parameter of the belonging atoms; in some cases their coordinates were blocked during the refinement process by means of DFIX instruction. One of the molecules of **HL**⁵ was highly disordered and the atoms of one of the aromatic rings were difficult to locate, and thus they were included in the model by means of the AFIX instruction. SIMU and DELU restrains had to be used in this case to make the ADP values of the atoms more reasonable. The data collection and refinement parameters are given in Tables S1 and S2, while a comparison of selected bond distances and angles are shown in Table 1. The perspective views of the molecular structures are shown in Figs. 1 and 2. No publishable results could be derived from the observed diffraction data for compounds **2** and **6**, however the raw data appear to indicate a tetrahedral structure.

Experimental protocol and cytotoxicity tests

Cell line maintenance and determination of IC₅₀ value

HeLa, MDA-MB-231 and HEK293 (human embryonic kidney) cells were obtained from National Centre for Cell Science (NCCS), Pune, India and were grown in Dulbecco Modified Eagle Medium (DMEM) with L-glutamine which was supplemented with penicillin, streptomycin and 10% FBS (Fetal Bovine Serum). Cells were maintained at 37°C in a humidified atmosphere containing 5% CO₂. Cells were harvested at 80-90% confluence and plated for subsequent experiments.

The cell viability was checked by the MTT assay (colorimetric assay) based on the conversion of the yellow tetrazolium salt MTT to purple formazan crystals after reaction with mitochondrial dehydrogenase of metabolically active cells.⁴⁸ Stock solutions (1 mM) of pro-ligands HLⁿ (n = 1-8), 3-(phenylamino)isobenzofuran-1(3H)-one and 3-((4-fluorophenyl)amino)isobenzofuran-1(3H)-one, and compounds **1-11** were prepared in DMSO and diluted with DMEM (a culture medium comprising 10% fetal bovine serum, supplemented with 20 mM L-glutamine, 100 units per mL penicillin and 100 µg mL⁻¹ streptomycin) such that the final concentration of DMSO did not exceed 0.1% v/v. CDDP stock solution (1 mM) was prepared in normal saline (0.9% sodium chloride).

The cytotoxic activities of HLⁿ, Phthalide-H, Phthalide-F and **1-11** were tested against HeLa, MDA-MB-231 and HEK293 cells at varying concentrations ranging from 0.2 to 2.0 µM. Cells were seeded in three different 96-well flat-bottom plates, keeping a similar cell density of around 8×10³ in each well, supplemented with complete media and incubated overnight to adhere under a humidified atmosphere at 5% CO₂.

The adhered cells were further treated with predefined concentrations of compounds and CDDP, then incubated further for 24 h in 5% CO₂ humidified atmosphere. The medium was then discarded and 100 µL of fresh medium and 10 µL (5 mg mL⁻¹) MTT in phosphate buffered saline, PBS (pH 7.4) added to each well and incubated further for 2 h. Finally, 100 µL of DMSO was added to each well to dissolve the insoluble purple MTT formazan crystals followed by incubation for 30 min. Similarly; the MDA-MB-231 and HeLa cells were exposed to various concentrations of CDDP as the drug control. The absorbance of samples was measured after 30 min at 570 nm using an ELISA plate reader. The per cent cell inhibition was calculated with respect to control and IC₅₀ (inhibitory concentration) values obtained were represented as mean ± SD for triplicates.

Hoechst 33342/PI assay

Hoechst 33342 dye is cell permeable and binds to DNA in live or dead cells, while PI is cell membrane impermeable so is excluded from the viable cells and typically used to identify dead cells. For this

experiment, HeLa cells (2×10^5) were seeded in 6 well plates and kept for 24 h at 37 °C in a humidified atmosphere of 5% CO₂. Thereafter, cells were treated with 0.2, 0.4 and 0.6 μM concentrations of **1** and **5** for 24 h at 37 °C. Subsequently, the medium was removed and cells were washed with 1 × PBS, stained with Hoechst 33342 (10 μg mL⁻¹) and PI (15 μg mL⁻¹) solutions and incubated at 37 °C for 30 min in the dark. After incubation, the cells were washed with PBS and images of nuclear morphology of living and apoptotic cells were captured using an inverted fluorescent microscope in red and blue channels as well as in phase contrast.

ROS generation assay

The ROS assay was carried out to determine the influence of the triphenyltin compounds **1** and **5** on the production of ROS levels in treated cells. The intracellular ROS level was assessed using DCFH-DA in HeLa and HEK 293 cells. DCFH-DA is a cell permeable dye, which is hydrolyzed by cellular esterase to non-fluorescent form and is oxidized and converted to fluorescent DCF in presence of ROS. Briefly, HeLa and HEK 293 cells were seeded in two different 6 well plates at a density of around 4×10^5 cells per well for 24 h at 37 °C in a humidified atmosphere of 5% CO₂. Then, both HeLa and HEK 293 cells were treated with concentrations of 0.2, 0.4 and 0.6 μM (within the IC₅₀ range) of compounds **1** and **5** for 24 h at 37 °C maintaining the humidified atmosphere of 5% CO₂. The treated cells were washed with PBS and then exposed in DCFH-DA dye (10 μM) for 25 min at 37 °C. The treated cell samples, along with control, were subjected to inverted fluorescence microscopy and DCF fluorescence was detected ($\lambda_{\text{ex}} = 485 \text{ nm}$; $\lambda_{\text{em}} = 530 \text{ nm}$) and then images were captured.

Cell cycle analysis

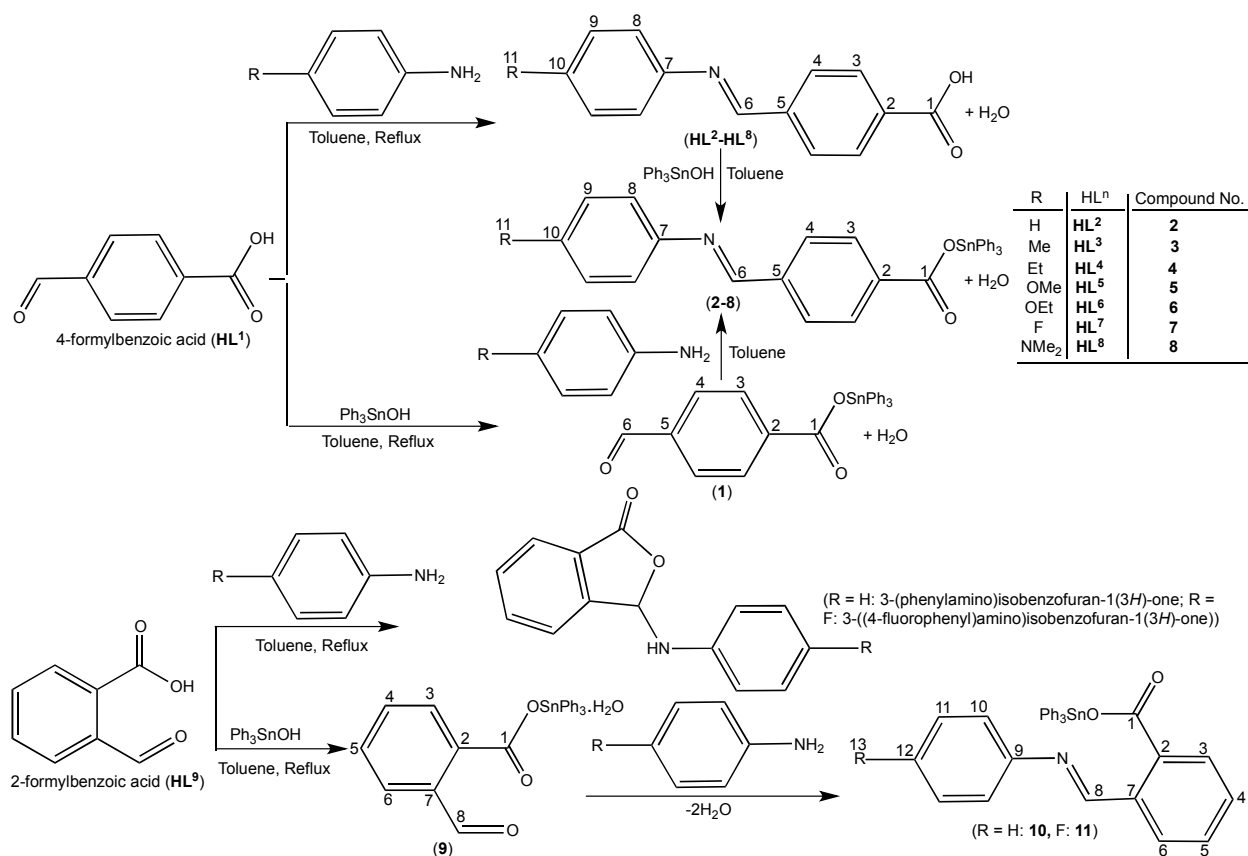
The effect of the triphenyltin(IV) compounds **1** and **5** on cell cycle distribution was evaluated by flow cytometry analysis of cellular DNA content through the PI staining. HeLa cells (4×10^5) were seeded in 6 well plates as described above, and then treated with IC₅₀ concentrations of **1** and **5** for 24 h in DMEM with 10% FBS. Cells were then washed, trypsinized and fixed in ice-cold 70% ethanol and kept overnight at -20

°C. The cells were washed twice in ice-cold PBS, then stained by 500 μL of staining solution (0.1% (v/v) Triton X-100 solution, PI (1 mg mL^{-1}) solution and RNase (10 mg mL^{-1} in PBS) and incubated for 30 min at 37 °C in the dark. After the staining procedure, cell samples were assessed and the cell cycle distribution was analyzed using a FACS Aria II flow cytometer and CELLQUEST software (Becton Dickinson).

Results and discussion

Synthesis and general aspects

The stereochemistry of the metal ions in Schiff base complexes can be tuned by introducing suitable groups into the ligand precursors. Accordingly, triphenyltin(IV) compounds **2-8** were prepared either by reacting (*E*)-4-((phenylimino)methyl)benzoic acid ($\text{HL}^2\text{-HL}^8$) with Ph_3SnOH or by condensing triphenylstannyl 4-formylbenzoate [$\text{Ph}_3\text{Sn}(\text{L}^1)$] (**1**) with appropriate anilines. In the present investigation, the synthetic conveniences led to the choice of the later method. In contrast to *para*- derivatives, synthesis of (*E*)-2-((phenylimino)methyl)benzoic acid (HL^{11}) and (*E*)-2-(((4-fluorophenyl)imino)methyl)benzoic acid (HL^{12}) could not be accomplished because equimolar reactions of aniline and *p*-fluoroaniline with 2-formylbenzoic acid in refluxing toluene proceeded via cyclization to give 3-(phenylamino)isobenzofuran-1(3H)-one (Phthalide-H) and 3-((4-fluorophenyl)amino)isobenzofuran-1(3H)-one (Phthalide-F), respectively (refer to note in the experimental section and see refs. 42 and 43). Therefore, compounds **10** and **11** were prepared by reacting aqua-triphenylstannyl 2-formylbenzoate [$\text{Ph}_3\text{Sn}(\text{L}^9)(\text{H}_2\text{O})$] (**9**) with appropriate anilines. Apparently, the generation of iminobenzoate ligands, e.g., (*E*)-2-((phenylimino)methyl)benzoate (L^{11}) and (*E*)-2-(((4-fluorophenyl)imino)methyl)benzoate (L^{12}) can be promoted by the reactions of **9** with aniline and *p*-fluoroaniline, respectively, which prevented the formation of cyclized product phthalides. Synthetic avenues towards the preparation of the aforementioned compounds **1-11** are detailed in Scheme 1.



Scheme 1. The synthetic methodologies for obtaining pro-ligands and triphenyltin compounds produced from the reactions thereof (1-11), along with numbering protocol of ligand framework used for NMR signal assignment.

The triphenyltin(IV) compounds **1-11** are soluble in common organic solvents, furnishing single crystals of the representative compounds suitable for diffraction studies and the congruence of all analytical data served to identify the composition. Behavior of the ligands in the presence of metal centres with different coordination geometries and numbers of available coordination sites was assessed from the results of spectroscopic and X-ray diffraction data. Pro-ligands have been characterized by IR, ^1H and ^{13}C spectroscopic techniques, while additionally ^{119}Sn NMR was used for the triphenyltin compounds. IR bands of the compounds along with the assignment of $\nu(\text{OCO})_{\text{asym}}$ and $\nu(\text{C(H)=N})$ have been presented in the experimental section. In the IR spectra of **2-8**, the asymmetric stretching $\nu(\text{OCO})_{\text{asym}}$ vibration for the ligands were detected in the range $1675\text{-}1685\text{ cm}^{-1}$, which is $\sim 60\text{ cm}^{-1}$ lower than those found for the respective pro-ligands due to coordination of the carboxylate group to the tin atoms.⁴⁹ The shift of $\nu(\text{OCO})_{\text{asym}}$ vibration is more pronounced in the case of compounds of *ortho*-analogues **10** and **11**. All compounds displayed anticipated ^1H and ^{13}C signals for the ligand and Sn-Ph moieties, which are given in the experimental section. The ^1H and ^{13}C chemical shift assignment of the phenyltin moiety is straightforward from the multiplicity patterns, resonance intensities and also by examining the $^nJ(^{13}\text{C}\text{-}^{119/117}\text{Sn})$ coupling constants.⁴⁹⁻⁵¹ The ^{119}Sn NMR spectra of compounds **1-11** displayed a single sharp ^{119}Sn resonance in the range at *ca.* -98 to -107 ppm, indicative of a four-coordinated tin coordination geometry in CDCl_3 solution, in accordance with the literature precedents.^{50,51} This observation suggests that the Sn-atom geometries observed in the solid-state for compounds **8**, **10** and **11** (tetragonal) and **9** (*trans*-trigonal bipyramidal) dissociate in solution to give rise to a tetrahedral geometry (see X-ray discussion, *vide infra*).

Description of the crystal structures

The pro-ligands (**HL**³, **HL**⁵ and **HL**⁶) and representative triphenyltin compounds **5**, **7-11** were authenticated by single-crystal X-ray diffraction. Crystal data and structure refinement parameters are given in Tables S1 and S2, while Tables 1 and 2 present a comparison of selected geometrical parameters. Figs. 1 and 2 display the molecular structures of the pro-ligands and triphenyltin compounds. Relevant intermolecular interactions for **5**, **7**, **8**, **9**, **11** and **HL**³ are shown in Figs. S1-S5, ESI.†

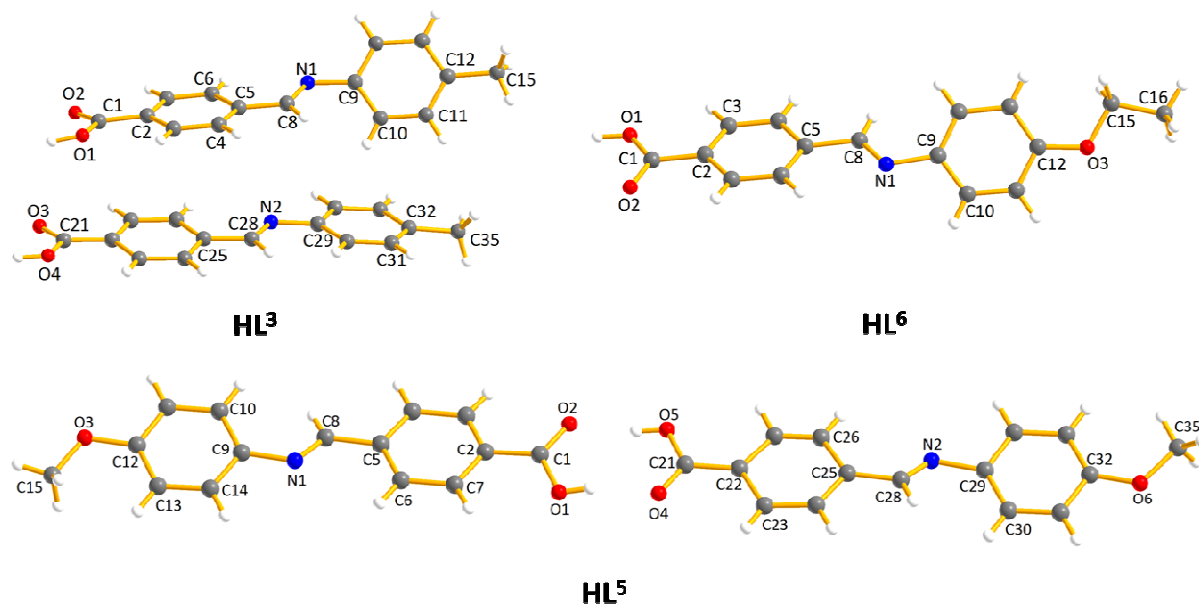


Fig. 1 Perspective views of the molecular structures of HL³, HL⁵ and HL⁶ with partial atom labeling schemes.

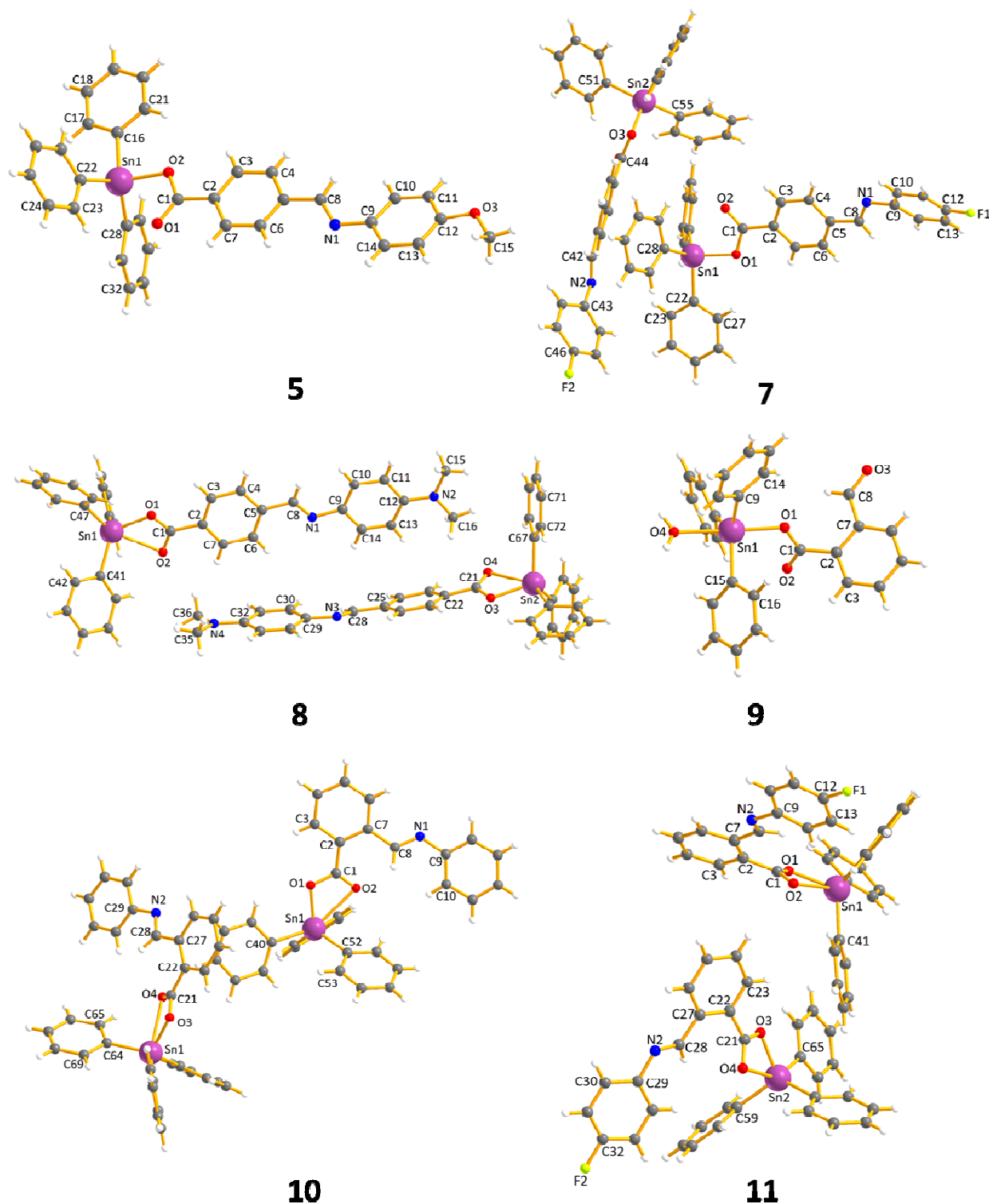


Fig. 2 Perspective views of the asymmetric units of [Ph₃Sn(L⁵)] (5), [Ph₃Sn(L⁷)] (7), [Ph₃Sn(L⁸)] (8), [Ph₃Sn(L⁹)(H₂O)] (9), [Ph₃Sn(L¹⁰)] (10) and [Ph₃Sn(L¹¹)] (11) with partial atom labeling schemes.

The asymmetric units of **5** and **9** contain one molecule of the complex but those of **7**, **8**, **10** and **11** comprise two crystallographically independent molecules. The metal cations in **5** and **7** present slightly distorted tetrahedral geometries (τ_4 of 0.89 and 0.92, respectively)⁵² while those of **8-11** are better described as distorted tetragonal (τ_5 between 0.46 and 0.56 for **8**, **10** and **11**)⁵³ or trigonal bipyramid (**9**, $\tau_5 = 0.90$). The criterion to judge between these two geometries was based on the Sn–O_{carboxylate} bond distances; while the shorter distances range from 2.047(4) to 2.096(8) Å and achieve 2.1656(14) Å in **9** (Table 1), the longer distances vary between 2.567(9) and 2.772(2) Å [**9** is the exception, with 2.3804(15) Å]. In compounds **5-7** the dimensions range from 2.803(3) to 2.855(4) and were thus treated as Sn···O contact distances. The Sn–C bond distances are in the usual range for Sn(IV) compounds⁵⁴⁻⁵⁸ and the C_{imino}–N lengths [1.242(13)-1.390(13) Å] prove the double bond character of the bond.

The phenyliminomethyl benzoate or benzoic groups are generally not planar as measured by the C_{imino}NC_{Ar}C_{Ar} torsion angle (Tables 1 and 2), which assume values as low as –142.3° in one of the molecules of HL³, –149.6° in HL⁶ or even –139.6° in one of the molecules of **7**. In the remaining triphenyltin compounds, such values range from 153° (in **7**) to 173° (in **8**). The carboxylic groups and attached aromatic rings are coplanar in the pro-ligands, however the carboxylate moieties and aromatic rings can be highly twisted in the compounds. For example, in **9** such groups are nearly orthogonal (O_{Sn}CC_{Ar}C_{Ar} torsion angle of 118.9°), but this geometric parameter increases to close to 170° in some cases (Table 1).

Structures of the compounds are stabilized by intermolecular non-covalent interactions, such as $\pi \cdots \pi$ stacking. In **5**, the molecules are gathered in pairs by means of almost perfectly aligned aromatic rings of the L[–] ligands, whose *centroids* are 3.742 Å apart (Fig. S1, ESI.†). Face-to-face orientations were also observed in **8**, though less intense (*centroid*···*centroid* distance of 3.923 Å, Fig. S2, ESI.†) and involving the phenyl groups bound to tin, and in **9** (*centroid*···*centroid* distance of 3.747 Å, Fig. S3, ESI.†) linking the formylbenzoate rings. In **7**, the aromatic rings are parallel displaced and comprise the L[–] ligand and a

phenyl group (*centroid*···*centroid* distance of 3.937 Å, Fig. S2, ESI.†), respectively. C–H··· π contacts in **8** are intense and reach values of 2.866 and 2.937 Å in the latter (Figs. S2, ESI.†). Resulting from the F-substituted aromatic ring in the L⁻ ligand of **11**, the Sn1 and the Sn2 containing molecules are coupled by means of C–F··· π connections involving the benzoate rings (C–F···*centroid* of 3.726 and 3.630 Å, respectively; Fig. S4, ESI.†). Only one of such type of contact was found in **7** (Fig. S2, ESI.†) covering a longer distance (3.916 Å) and involving one of the Sn-bound phenyl groups. In the structure of **HL**³, two types of molecules are assembled by means of both the π ··· π and the C–H··· π interactions (*centroid*···*centroid* and H···*centroid* distances of 4.007 and 2.856 Å, in this order), the latter resulting from the relative orientations of the aromatic rings (Fig. S5, ESI.†). Concerning the intermolecular Sn···Sn distance, the compounds follow the order (Table 2): **7** [8.3258(5) Å] > **11** [8.0131(7) Å] > **5** [7.827(1) Å] > **9** [7.4569(4) Å] > **10** [7.2296(5) Å] > **8** [7.173(1) Å].

Table 1 Sn coordination geometry and selected geometrical parameters for the triphenyltin compounds **5**, **7-11**

Parameters	Compounds					
	5	7	8	9	10	11
Tin coordination number	4	4	5	5	5	5
Tin coordination sphere ^a and geometry indices	Tetrahedral ($\tau_4 = 0.89$)	Tetrahedral ($\tau_4 = 0.91$) (Sn1) ($\tau_4 = 0.92$) (Sn2)	Dist. tetragonal ($\tau_5 = 0.48$) (Sn1) ($\tau_5 = 0.52$) (Sn2)	Trigonal bipyramid ($\tau_5 = 0.90$)	Dist. tetragonal ($\tau_5 = 0.56$) (Sn1) ($\tau_5 = 0.48$) (Sn2)	Dist. tetragonal ($\tau_5 = 0.49$) (Sn1) ($\tau_5 = 0.46$) (Sn2)
Sn–O [Sn \cdots O] (Å)	2.058(3) [2.803(3)]	2.062(4) (Sn1) [2.831(4)] 2.047(4) (Sn2) [2.855(4)]	2.096(8) (Sn1) 2.567(9) Sn1 2.072(7) (Sn2) 2.725(8) (Sn2)	2.1656(14) 2.3804(15)	2.076(2) (Sn1) 2.647(2) (Sn1) 2.058(2) (Sn2) 2.772(2) (Sn2)	2.081(3) (Sn1) 2.726(3) (Sn1) 2.087(3) (Sn2) 2.674(3) (Sn2)
Sn–C (°)	2.121(5) - 2.130(5)	2.108(7) - 2.137(6) (Sn1) 2.121(6) - 2.134(6) (Sn2)	2.125(13) - 2.136(13) (Sn1) 2.123(11) - 2.127(13) (Sn2)	2.118(2) - 2.1341(19)	2.121(3) - 2.139(3) (Sn1) 2.115(3) - 2.130(3) (Sn2)	2.119(4) - 2.122(4) (Sn1) 2.117(4) - 2.125(4) (Sn2)
N=C (Å)	1.249(7)	1.266(8) 1.253(7)	1.242(13) 1.390(13)	-	1.256(4)	1.270(5) 1.252(5)
\angle O _{Sn} CC _{Ar} C _{Ar} (°)	178.1	-164.3 (Sn1) -167.4 (Sn2)	Avg. 168 (Sn1) Avg. 163 (Sn2)	118.6	Avg. 155 (Sn1 and Sn2)	-144.8, -138.9 (Sn1) 145.9, 138.8 (Sn2)
\angle C _{imino} NC _{Ar} C _{Ar} (°)	163.0	-153.0 (Sn1) -139.6 (Sn2)	173 (Sn1) 168 (Sn2)	-	-155.1 (Sn1) 158.9 (Sn2)	157.8 (Sn1) -154.0 (Sn2)
Intermolecular Sn \cdots Sn (minimum)	7.827(1)	8.3258(5)	7.173(1)	7.4569(4)	7.2296(5)	8.0131(7)

^a For the definition of τ_4 and τ_5 , see references [52,53].

Table 2 Selected geometrical parameters for the pro-ligands **HL**³, **HL**⁵ and **HL**⁶

Parameters	Pro-ligands		
	HL ³	HL ⁵	HL ⁶
N=C (Å)	1.259(3) 1.243(3)	1.281(10) 1.19(4)	1.198(5)
∠ C _{imino} NC _{Ar} C _{Ar} (°)	-142.3 174.1	160.6 -159	-149.6
D-H...A [d _{D...A} (Å); ∠(D-H...A) (°)]	O1-H1O...O3 [2.618(2); 173(3)] O4-H4O...O2 [2.636(2); 175(3)]	O1-H1...O4 [2.646(17); 168] O5-H5...O2 [2.58(2); 171]	O1-H1O...O2 [2.633(3); 171(5)]

Solubility and stability assessment of triphenyltin(IV) compounds 1-11

The triphenyltin(IV) compounds (**1-11**) are soluble in acetonitrile, DMF and dimethylsulfoxide (DMSO), acetone, methanol, ethanol, dichloromethane, chloroform, xylene and toluene but insoluble in hexane. The solution stability of a drug under physiological conditions is an important pre-requisite for its *in vitro/ in vivo* applications. Usually, organotin(IV) compounds are dissolved in DMSO and diluted with test medium prior to *in vitro* testing and hence the stabilities of the triphenyltin(IV) compounds **1-11** were assessed by UV-visible spectroscopy in DMSO prior to the cytotoxic studies. The compounds were found to be stable, as evidenced from the unchanged basic pattern of absorption spectra even after 21 days (Fig. S6, ESI[†]).

Evaluation of *in vitro* cytotoxicity

Effective concentrations to affect cell viability

The effectiveness of triphenyltin(IV) compounds in suppressing tumor cells and advancing apoptosis has been well established.^{8-12,22} The overall goal of the present investigation was to synthesize chemopreventive agents that could potentially lead to their use in clinical evaluation. Having now the availability of a well-characterized series of pro-ligands (HLⁿ) and triphenyltin compounds **1-11**, it is possible to make a direct comparison of their anti-cancer efficacy. To this end, the anti-proliferative/apoptotic activity of compounds **1-11** described above was evaluated against human HeLa, MDA-MB-231 cancer cells and normal HEK 293 cells. Explicitly, to first determine in which concentration range these compounds mediate cytotoxic effects; we conducted an *in vitro* cytotoxicity screen in HeLa, MDA-MB-231 and HEK 293 cells (Figs. S7-S9 ESI[†]) and compared the effects with an untreated control, triorganotin(IV) precursor Ph₃SnOH (Fig. S10, ESI[†]) and CDDP using the MTT assay after incubation of 24 h. IC₅₀ values (μM) for pro-ligands (HLⁿ), Phthalide-H and Phthalide-F and triphenyltin compounds **1-11** in studied cells are given in Table 3. As shown in Fig. S11, ESI[†], all

Table 3 IC₅₀ values (μM) for triphenyltin compounds **1-11** and CDDP after 24 h exposure in cancer cells (HeLa, MDA-MB-231) and normal HEK 293 cells

Test compounds ^a	IC ₅₀ values (μM) ± SE ^b		
	HeLa	MDA-MB-231	HEK 293
Ph ₃ Sn(L ¹) (1)	0.51±0.02	0.76±0.25	1.28±0.04
Ph ₃ Sn(L ²) (2)	0.23±0.03	0.77±0.06	1.15±0.03
Ph ₃ Sn(L ³) (3)	0.19±0.00	0.97±0.14	0.71±0.02
Ph ₃ Sn(L ⁴) (4)	0.63±0.05	0.62±0.12	0.36±0.04
Ph ₃ Sn(L ⁵) (5)	0.41±0.08	0.78±0.03	1.46±0.03
Ph ₃ Sn(L ⁶) (6)	0.24±0.09	0.75±0.05	2.3±0.02
Ph ₃ Sn(L ⁷) (7)	0.27±0.01	0.75±0.02	0.72±0.02
Ph ₃ Sn(L ⁸) (8)	0.45±0.01	0.51±0.09	0.74±0.04
Ph ₃ Sn(L ⁹) (9)	0.41±0.01	0.44±0.03	0.41±0.02
Ph ₃ Sn(L ¹⁰) (10)	0.72±0.08	0.43±0.00	1.35±0.03
Ph ₃ Sn(L ¹¹) (11)	0.53±0.09	0.39±0.12	1.22±0.03
Ph ₃ SnOH	0.52±0.04	0.42±0.09	1.96±0.02
CDDP	51.3±1.19	23.63±0.20	c

^aCytotoxicity of the pro-ligands HL¹-HL⁹, Phthalide-H and Phthalide-F were found to be non-toxic up to tested concentration of 2 μM as the viability of cells were 90%.

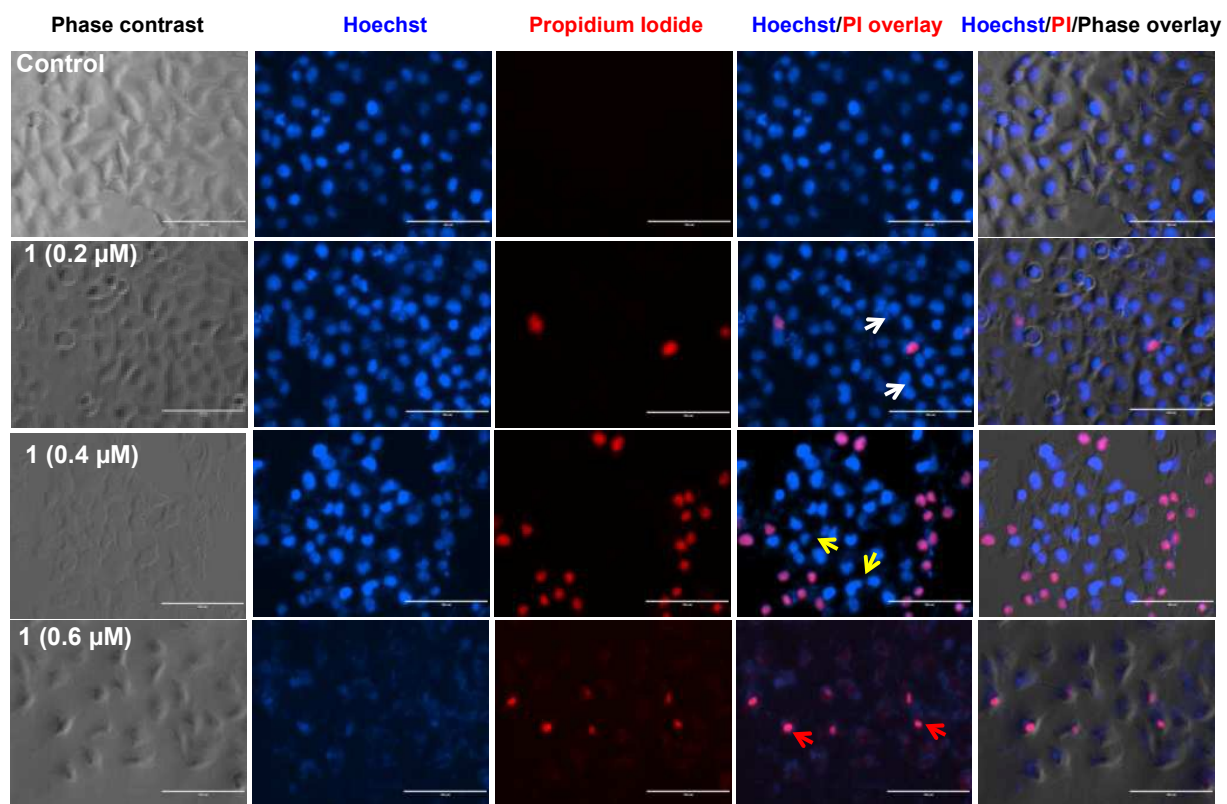
^bStandard error and the value represents the average of three sets of independent experiments.

^cNot determined.

pro-ligands (HL¹-HL⁹), Phthalide-H and Phthalide-F exhibited no toxic effect up to the tested concentration of 2 μ M (shown up to 1 μ M in Fig. S11). While no significant change can be observed for the IC₅₀ values of HLⁿ, Phthalide-H and Phthalide-F, a marked increase in the sub-micromolar concentration range of the respective compounds **1-11** against the cells were noted. Thus, the experiential greater toxicities can apparently be correlated due to the manifestation of three phenyl ligands, which impart higher lipophilic character in **1-11** than that of their corresponding HLⁿ, which facilitates binding to biological molecules by π ... π interaction.⁵⁹ However, the maximal differential effect among the compounds is exhibited by **3** in HeLa cells and **11** in MDA-MB-231 cells, and the IC₅₀ value drops to 0.19 μ M and 0.39 μ M, respectively, thus becoming the most cytotoxic compound among those tested with respect to both the control conditions. Although compounds **3**, **6** and **7** exhibit greater toxicity in cancer cells, they also induced significant toxicity in normal cells, and hence further studies with these compounds were not conducted. Among the test compounds included in the present investigation, **1** and **5** displayed significant inhibitory effects in both HeLa and MDA-MB-231 cells in a dose-dependent manner and they were found to be more potent than the clinically used drug CDDP. However, **1** and **5** show maximum inhibition in HeLa cells and the encouraging IC₅₀ values prompted the determination of their cytotoxicity towards normal human kidney cells (HEK 293) which indeed did not induce cytotoxicity even at higher concentration (Fig. S9, ESI[†]). The triphenyltin compound **1** exhibited lower cytotoxic effects in comparison with **5**. Such variations in cytotoxic effects might be attributed to differences in the chemical structures (molecular weight) of the molecules of **1** and **5** (additional benzene ring connected via imino bond) and hydrophobicity, leading to variation in the cellular uptake.⁶⁰ Based on these criteria, further biological experiments were conducted to ascertain the modes of cell death induced by **1** and **5** in HeLa cells. The tested compounds and CDDP showed concentration-dependent cytotoxic effects.

Assessment of cellular and nuclear morphological changes during apoptosis

The apoptotic mode of cell death leads to distinct morphological and biochemical features, which are accompanied by nuclear shrinkage, cytoplasmic membrane blabbing, chromatin condensation, fragmentation of the nucleus, etc.^{61,62} As compounds **1** and **5** exhibited convincing inhibitory effects, it became vital to visualize the nuclear morphology and membrane integrity during the course of apoptosis. For this purpose, the HeLa cells have been treated with 0.2, 0.4 and 0.6 μM concentrations of compounds **1** and **5** for 24 h and then Hoechst 33342 and PI staining (DNA binding dyes) was employed. Selected fluorescence microscopy images are shown in Figs. 3 (a) and 3 (b) wherein the white, yellow and red arrows indicate early apoptotic, late apoptotic and necrotic (nuclei) cells, respectively. Image analysis revealed that both the compounds induced apoptotic cell death upon treatment on HeLa cells. Untreated cells display normal nuclear morphology with uniform light blue nucleus, whereas compounds treated cells display distinct apoptotic nuclear morphology with condensed bright blue nucleus. Further treatment of HeLa cell with higher IC_{50} concentration of the compounds increased the occurrence of apoptotic nuclei and thus results also indicated that apoptotic cell death increases in a dose-dependent manner compared to the control.

(a)

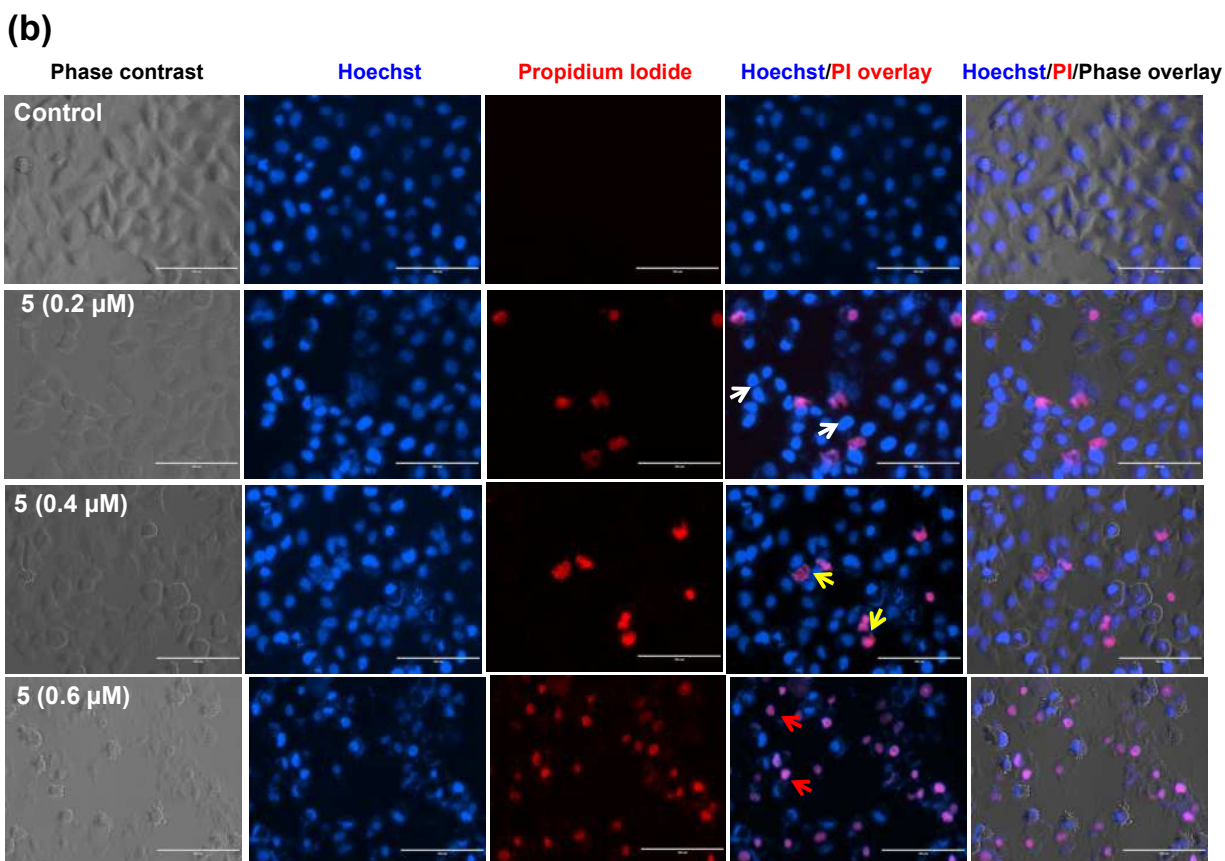


Fig. 3 Fluorescence microscope images showing morphological (nuclear) changes in HeLa cells upon treatment with specified concentrations of (a) compounds **1** and (b) **5**, respectively, by dual staining with Hoechst 33342 and PI for 24 h. The white, yellow and red arrows indicate early apoptotic, late apoptotic and necrotic, respectively.

ROS generation

The generation of intracellular ROS and mitochondria play an important role in apoptosis induction under both physiological and pathological conditions.⁶³ Small molecule ROS generators have shown a lot of success in the therapeutic arena and in this quest, organotin(IV) compounds are known to induce apoptosis by increasing the intracellular ROS level.^{22,64} To examine and visualize the generation of intracellular ROS by compounds **1** and **5**, the DCFH-DA assay was performed. DCFH-DA, the non-fluorescent ROS marker hydrolyzes to 2',7'-dichlorodihydrofluorescein (DCFH) in live cells which in turn, upon oxidation by ROS, gets converted to the highly green fluorescent 2',7'-dichlorofluorescein (DCF).^{65,66} The generation of ROS was evaluated for HeLa cells treated with only DCFH-DA and for cells treated with DCFH-DA and compounds **1** and **5**, both with 0.2, 0.4 and 0.6 μM concentrations. The green fluorescence of DCF was found to be significantly higher in compound treated cells in comparison with control, signaling that triphenyltin compounds (**1** and **5**) are responsible for the generation of ROS. As can be seen in Fig. 4, ROS production increases in a dose-dependent manner compared to the control. The generation of ROS was also examined in normal HEK 293 cells at the IC_{50} concentration of **1** and **5** obtained against HeLa cells. In general, both compounds **1** and **5** did not induce increased ROS production in HEK 293 cells (Fig. S12, ESI[†]), as compared to the HeLa cancer cells (Fig. 4) besides a few cells showing basal ROS induction. These data argue for a possible involvement of ROS as upstream molecular components in the apoptotic effect of triphenyltin compounds **1** and **5** that can induce oxidative stress in HeLa cells. Prior art indicated that tin organometallics could act as a ROS generator to increase the susceptibility of tumor cells to apoptosis.^{22,67}

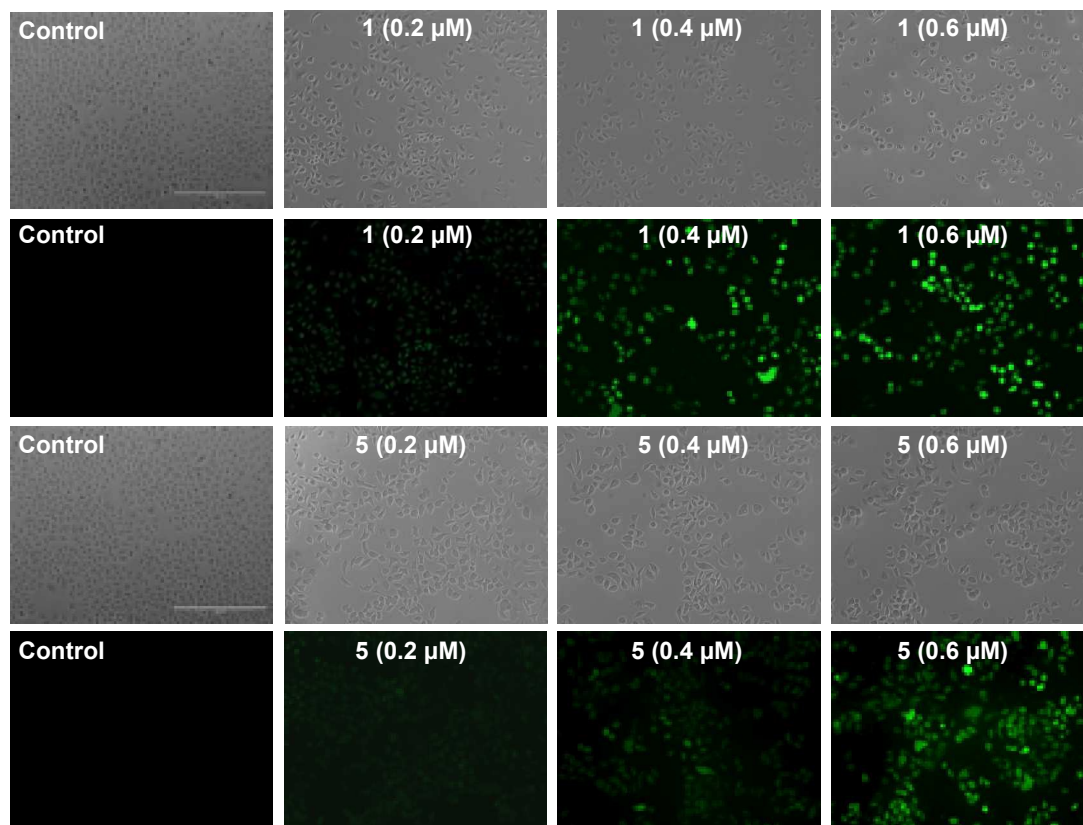


Fig. 4 Dose-dependent generations of ROS after 24 h treatment with IC_{50} concentrations of **1** and **5** in HeLa cells, detected through DCFH-DA fluorescence staining dye by measuring the fluorescence intensity viewed through fluorescence microscope.

Cell cycle arrest studies

It is known that the deregulation of cell cycle progression leading to the uncontrolled cell growth arrest and over proliferation of the cells play a critical role in cancer initiation and progression.⁶⁸ Based on encouraging results described above, we further investigated the possible mechanism of action of compounds **1** and **5** in order to record changes on the cell cycle phase distribution on the basis of DNA content in HeLa cells by flow cytometry analysis using PI staining.⁶⁹ The cells were treated with the concentrations close to the IC₅₀ values determined for **1** and **5** and the observed FACS histogram statistics are recorded in Fig. 5 (refer to Fig. S13, ESI† for bar chart). For instance, the treatment of HeLa cells with compound **1** induces a marginal increase in cell cycle arrest from 16.8% (control cells) to 21.7% (treated cells) particularly in G2/M and sub-G1 phases while no notable changes were observed at the S phase of the cell cycle, at IC₅₀ concentration. On the other hand, when the cells were treated with variable concentrations of **5**, a decrease in cell population from 51.6% to 35% in G1 phase was noted, although the percentage of apoptotic cells increased substantially from 2.9% to 18% at sub-G1 phase while a marginal change from 9.8% to 13.4% of apoptotic cells were noted at 0.6 μM concentration. Thus, FACS histogram statistics clearly revealed that **5** resulted in more evident changes in the cell cycle than **1**, and that the antiproliferative mechanism of **1** and **5** on HeLa cells is dominantly G1 and G2/M phase arrests and were concentration dependent.

The antiproliferative activities of compounds **1-11** are much higher than that of the pro-ligands, suggesting that the significantly higher anticancer activity is due to the complexation with Sn(IV) phenyl moieties. Notably, the activities of compounds **1** and **5** are much higher with IC₅₀ values for cell growth proliferation 100-125 times larger than those of CDDP towards the HeLa cells. Studies show that the compounds activate the apoptotic mechanisms induced by the triphenyltin(IV) compounds depends on cell type, specificity and concentrations, which is mainly prompted by apoptosis via ROS generation. Since the induction of apoptosis and cell growth arrest have been regarded as a new target in anticancer drug discovery, the present study confirmed the chemotherapeutic and cytotoxicity potential of compounds **1** and **5** in HeLa cells.

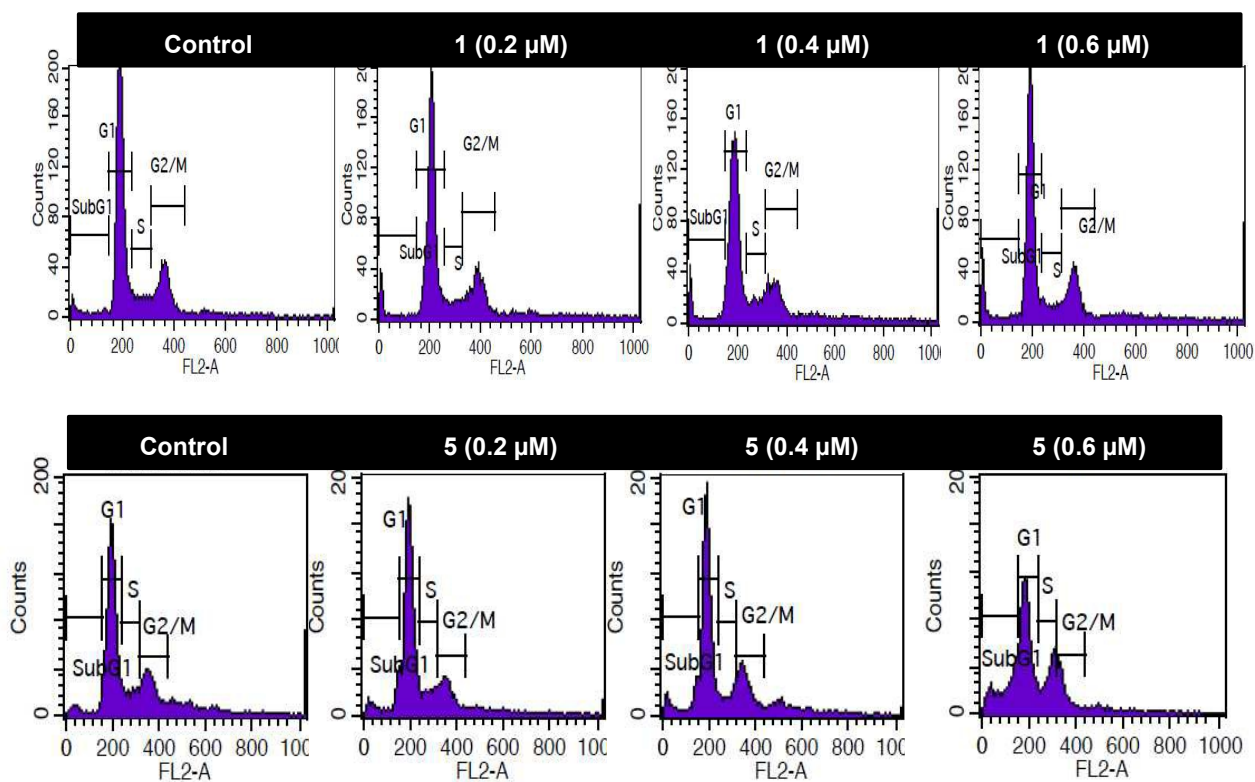


Fig. 5 Investigation of cell cycle delay on basis of DNA content through FACS analysis of PI-stained HeLa cancer cells after 24 h of exposure to concentrations of compounds **1** and **5**.

Conclusions

A series of eleven triphenyltin(IV) compounds were synthesized and characterized by elemental analysis and well-known spectroscopic techniques, with six of the tin compounds (**5**, **7-11**) and three pro-ligands (**HL**³, **HL**⁵ and **HL**⁶) characterized by single-crystal XRD analysis. In the crystalline state, these compounds generally adopt a four- or five-coordination mode, and the Sn(IV) atoms display a distorted tetrahedral geometry for **5** and **7**, distorted tetragonal geometry for **8**, **10** and **11**, and trigonal bipyramid geometry for **9**. Compounds **1-11** were tested *in vitro* against HeLa and MDA-MB-231 cells and showed remarkable cytotoxicity, in the low micromolar range of IC₅₀. Data showed that all the tin compounds exhibited pronounced *in vitro* cytotoxicity of the same order of magnitude, but much higher than CDDP toward both cells. Among others, compounds **1** and **5** were tested against HeLa while being considerably less toxic as they did not affect viability of normal HEK-293 cells, therefore showing high selectivity towards tumor cells, rather than to healthy cells. The cell cycle arrest studies by flow cytometry demonstrated that the antiproliferative effect induced by **1** and **5** on HeLa cells occurred in the G2/M phases. The apoptosis assay by Hoechst 33342 and PI staining showed that **1** and **5** effectively induced apoptosis of HeLa cells, and the number of apoptotic cells increased with increasing concentrations. Compounds **1** and **5** induce apoptosis by a mechanism involving the formation of ROS, as revealed from DCFH-DA assay. Thus, it may be inferred that inhibition of HeLa cell proliferation by **1** and **5** could be due to the combination of the induction of apoptosis and cell cycle arrest; moreover, the ROS generation by **1** and **5** may trigger the cell apoptosis. Further mechanistic studies are being planned and much work is needed to get insights into the structure-property relationship for their analogous compounds with enhanced efficacy, selectivity and a broad spectrum of activity.

Conflict of interests

The authors declare that they have no conflicts of interest with the contents of this article.

Acknowledgements

The financial support of the Council of Scientific and Industrial Research, New Delhi (Grant No. 01(2734)/13/EMR-II, 2013, TSBB), the University Grants Commission, New Delhi, India, through SAP-CAS, Phase-I and the Foundation for Science and Technology (FCT), Portugal (Project UID/QUI/00100/2013, MFCGS) is gratefully acknowledged. Authors (TSBB, IL) acknowledge DST-PURSE for the diffractometer facility. The authors (PS, BK) acknowledge financial support through UGC-CAS Phase-V and Interdisciplinary School of Life Sciences (ISLS), Institute of Science, Banaras Hindu University, for providing flow cytometry facility.

References

- 1 B. Rosenberg, L. VanCamp, J. E. Trosko and V. H. Mansour, *Nature*, 1969, **222**, 385-386.
- 2 P. R. Brock, K. R. Knight, D. R. Freyer, K. C. M. Campbell, P. S. Steyger, B. W. Blakley, S. R. Rassekh, K. W. Chang, B. Fligor, K. Rajput, M. Sullivan and E. A. Neuwelt, *J. Clin. Oncol.*, 2012, **30**, 2408-2417.
- 3 L. Kelland, *Nat. Rev. Cancer*, 2007, **7**, 573-584.
- 4 K. D. Mjos and C. Orvig, *Chem. Rev.*, 2014, **114**, 4540-4563.
- 5 W. A. Wani, S. Prashar, S. Shreaz and S. Gómez-Ruiz, *Coord. Chem. Rev.*, 2016, **312**, 67-98.
- 6 M. Gielen, in: M. Gielen, E.R.T. Tiekink (Ed.). *Metallotherapeutic Drug and Metal-based Diagnostic Agents: ⁵⁰Sn Tin Compounds and Their Therapeutic Potential*, Wiley, Chichester, England, 2005, pp. 421-439 and references therein.
- 7 S. K. Hadjikakou and N. Hadjiliadis, *Coord. Chem. Rev.*, 2008, **253**, 235-249.
- 8 M. K. Amir, S. Khan, Zia-ur-Rehman, A. Shah and I.S. Butler, *Inorg. Chim. Acta*, 2014, **423**, 14-25.
- 9 F. Arjmand, S. Parveen, S. Tabassum and C. Pettinari, *Inorg. Chim. Acta*, 2014, **423**, 26-37.
- 10 C. E. Carraher Jr. and M. R. Roner, *J. Organomet. Chem.*, 2014, **751**, 67-82.
- 11 L. Niu, Y. Li and Q. Li, *Inorg. Chim. Acta*, 2014, **423**, 2-13.
- 12 A. G. Davies, M. Gielen, K. H. Pannell and E. R. T Tiekink (Ed.). *Tin Chemistry Fundamentals, Frontiers and Application*, Wiley, Chichester, UK, 2008.
- 13 L. Plasseraud, D. Ballivet-Tkatchenko, H. Cattey, S. Chambrey, R. Ligabue, P. Richard, R. Willem and M. Biesemans, *J. Organomet. Chem.*, 2010, **695**, 1618-1626.
- 14 E. Arkis, in: A. G. Davies, M. Gielen, K. H. Pannell and E. R. T Tiekink (Ed.), *Organotin compounds as PVC stabilizers, Tin Chemistry Fundamentals, Frontiers and Application*, Wiley, Chichester, UK, 2008, pp. 312-323 and references therein.
- 15 J. -F. Lascourreges, P. Caumette and O. F. X. Donard, *Appl. Organomet. Chem.*, 2000, **14**, 98-107.
- 16 E. S. F. Ma, W. D. Bates, A. Edmunds, L. R. Kelland, T. Fojo and N. Farrell, *J. Med. Chem.*, 2005, **48**, 5651-5654.

- 17 A. G. Quiroga, J. M. Pérez, C. Alonso, C. Navarro-Ranninger and N. Farrell, *J. Med. Chem.*, 2005, **49**, 224-231.
- 18 D. Pérez-Quintanilla, S. Gómez-Ruiz, Ž. Žižak, I. Sierra, S. Prashar, I. del Hierro, M. Fajardo, Z. D. Juranić and G. N. Kaluđerović, *Chem. Eur. J.*, 2009, **15**, 5588-5597.
- 19 G. N. Kaluđerović, H. Kommera, E. Hey-Hawkins, R. Paschke and S. Gómez-Ruiz, *Metallomics*, 2010, **2**, 419-428.
- 20 S. Gómez-Ruiz, G. N. Kaluđerović, S. Prashar, E. Hey-Hawkins, A. Erić, Ž. Žižak and Z. D. Juranić, *J. Inorg. Biochem.*, 2008, **102**, 2087-2096.
- 21 M. Z. Bulatović, D. Maksimović-Ivanić, C. Bensing, S. Gómez-Ruiz, D. Steinborn, H. Schmidt, M. Mojić, A. Korać, I. Golić, D. Pérez-Quintanilla, M. Momčilović, S. Mijatović and G. N. Kaluđerović, *Angew. Chem. Int. Ed.*, 2014, **53**, 5982-5987.
- 22 T. S. Basu Baul, D. Dutta, A. Duthie, R. Prasad, N. K. Rana, B. Koch and E. R. T. Tiekink, *J. Inorg. Biochem.*, 2017, **173**, 79-92.
- 23 N. Metzler-Nolte, *Bioorganometallics*, in: G. Jaouen (Eds.), Wiley-VCH, Weinheim 2006, p. 125.
- 24 N. Metzler-Nolte, *Comprehensive Organometallic Chemistry III*, in: G. Parkin (Eds.), Vol. 1, Elsevier, Amsterdam 2007, p. 883
- 25 N. Metzler-Nolte and K. Severin, *Concepts and Models in Bioinorganic Chemistry*, in: K.-B. Kraatz, N. Metzler-Nolte (Eds.), Wiley-VCH, Weinheim, 2006
- 26 W. A. Zoubi and Y. G. Ko, *Appl. Organometal. Chem.*, 2016; 1-12 doi: 10.1002/aoc.3574
- 27 W. A. Zoubi and Y. G. Ko, *J. Organomet. Chem.*, 2016, **822**, 173-188
- 28 P. Das and W. Linert, *Coord. Chem. Rev.*, 2016, **311**, 1-23.
- 29 C. P. Pradeep and S. K. Das, *Coord. Chem. Rev.*, 2013, **257**, 1699-1715.
- 30 C. R. Nayar and R. Ravikumar, *J. Coord. Chem.*, 2014, **67**, 1-16.
- 31 A. W. Jeevadason, K. K. Murugavel and M. A. Neelakantan, *Renew. Sust. Energ. Rev.*, 2014, **36**, 220-227.
- 32 Manju, N. Mishra and D. Kumar, *Russ. J. Coord. Chem.*, 2014, **40**, 343-357.

- 33 H. Vardhan, A. Mehta, I. Nath and F. Verpoort, *RSC Adv.*, 2015, **5**, 67011-67030.
- 34 D. Utreja, Vibha, S. Singh and M. Kaur, *Curr. Bioact. Compd.*, 2015, **11**, 215-230.
- 35 M. Andruh, *Dalton Trans.*, 2015, **44**, 16633-16653.
- 36 J. Yang, R. Shi, P. Zhou, Q. Qiu and H. Li, *J. Mol. Str.*, 2016, **1106**, 242-258 and references therein.
- 37 W. A. Zoubi, A. A. S. Al-Hamdani and M. Kaseem, *Appl. Organometal. Chem.*, 2016, **30**, 810-817.
- 38 I. P. Ejidike and P. A. Ajibade, *Rev. Inorg. Chem.*, 2015, **35**, 191-224.
- 39 J. L. Segura, M. J. Mancheño and F. Zamora, *Chem. Soc. Rev.*, DOI: 10.1039/c5cs00878f
- 40 (a) M. Langner, J. Gabrielska and S. Przystalski, *Appl. Organomet. Chem.*, 2000, **14**, 25-33; (b) B. Rózycka-Roszak, H. Pruchnik and E. Kamiński, *Appl. Organomet. Chem.*, 2000, **14**, 465-472; (c) A. Miszta, J. Gabrielska, S. Przystalski and M. Langner, *Appl. Organomet. Chem.*, 2005, **19**, 736-741; (d) A. Olzyska, M. Przybylo, J. Gabrielska, Z. Trela, S. Przystalski and M. Langner, *Appl. Organomet. Chem.*, 2005, **19**, 1073-1078.
- 41 L. Pellerito and L. Nagy, *Coord. Chem. Rev.*, 2002, **224**, 111-150.
- 42 D. D. Wheeler, D. C. Young and D. S. Erley, *J. Org. Chem.*, 1957, **22**, 547-556.
- 43 M. Odabaşoğlu and O. Büyükgüngör, *Acta Crystallogr., Sect. E*, 2006, **62**, o2943-o2944.
- 44 CrysAlisPro, Version 1.171.35.19, Agilent Technologies, Yarnton, Oxfordshire, England, 2010.
- 45 A. Altomare, M. C. Burla, M. Camalli, G. L. Cascarano, C. Giacovazzo, A. Guagliardi, A. G. G. Moliterni, G. Polidori and R. Spagna, *J. Appl. Cryst.*, 1999, **32**, 115-119.
- 46 G. M. Sheldrick, *Acta Crystallogr., Sect. A*, 2008, **64**, 112-122.
- 47 L. J. Farrugia, *J. Appl. Cryst.*, 2012, **45**, 84-854.
- 48 T. J. Mosmann, *J. Immunol. Methods*, 1983, **65**, 55-63.
- 49 T. S. Basu Baul, A. Paul, L. Pellerito, M. Scopelliti, A. Duthie, D. de Vos, R. P. Verma and U. Englert, *J. Inorg. Biochem.*, 2012, **107**, 119-128.
- 50 R. Willem, I. Verbruggen, M. Gielen, M. Bieseman, B. Mahieu, T. S. Basu Baul and E. R. T. Tiekink, *Organometallics*, 1998, **17**, 5758-5766.
- 51 J. Holeček, M. Nádvorník, K. Handlíř and A. Lyčka, *J. Organomet. Chem.*, 1983, **241**, 177-184.

- 52 L. Yang, D. R. Powell and R. P. Houser, *Dalton Trans.*, 2007, 955-964.
- 53 A. W. Addison, T. N. Rao, J. Reedijk, J. van Rijn and G. C. Verschoor, *J. Chem. Soc., Dalton Trans.*, 1984, 1349-1356.
- 54 T. S. Basu Baul, D. Dutta, A. Duthie and M. F. C. Guedes da Silva, *Inorg. Chim. Acta, Part 2*, 2017, **455**, 627-637.
- 55 T. S. Basu Baul, D. Dutta, A. Duthie, N. Guchhait, B. G. M. Rocha, M. F. C. Guedes da Silva, R. B. Mokhamatam, N. Raviprakash and S. Manna, *J. Inorg. Biochem.*, 2017, **166**, 34-48.
- 56 X. Shang, B. Zhao, G. Xiang, M. F. C. Guedes da Silva and A. J. L. Pombeiro, *RSC Advances*, 2015, **5**, 45053-45060.
- 57 X. Shang, X. Meng, E. C. B. A. Alegria, Q. Li, M. F. C. Guedes da Silva, M. L. Kuznetsov and A. J. L. Pombeiro, *Inorg. Chem.*, 2011, **50**, 8158-8167.
- 58 M. N. Xanthopoulou, S. K. Hadjikakou, N. Hadjiliadis, M. Kubicki, S. Skoulika, T. Bakas, M. Baril and I. S. Butler, *Inorg. Chem.*, 2007, **46**, 1187-1195.
- 59 D. B. Shpakovsky, C. N. Banti, E. M. Mukhatova, Y. A. Gracheva, V. P. Osipova, N. T. Berberova, D. V. Albov, T. A. Antonenko, L. A. Aslanov, E. R. Milaeva and S. K. Hadjikakou, *Dalton Trans.*, 2014, **43**, 6880-6890.
- 60 (a) M. D. Hall, S. Amjadi, M. Zhang, P. J. Beale and T. W. Hambley, *J. Inorg. Biochem.*, 2004, **98**, 1614-1624 (b) S. P. Oldfield, M. D. Hall and J. A. Platts, *J. Med. Chem.*, 2007, **50**, 5227-5237.
- 61 S. Kasibhatla and B. Tseng, *Mol. Cancer Ther.*, 2003, **2**, 573-580.
- 62 J. F. Kerr, *Toxicol.*, 2002, **181-182**, 471-474.
- 63 H. -U. Simon, A. Haj-Yehia and F. Levi-Schaffer, *Apoptosis*, 2000, **5**, 415-418.
- 64 Ž. Jakšić, in: A. Pagliarani, F. Trombetti and V. Ventrella (Ed.), *Biochemical and Biological Effects of Organotins*, Bentham Science Publishers, 2012.
- 65 H. Wang and J. A. Joseph, *Free Radical Biol. Med.*, 1999, **27**, 612-616.
- 66 A. Gomes, E. Fernandes and J. L. F. C. Lima, *J. Biochem. Biophys. Methods*, 2005, **65**, 45-80.

- 67 (a) E. -L. Liu, X. Du, R. Ge, T. -G. Liang, Q. Niu and Q. -S. Li, *Food Chem. Toxicol.*, 2013, **60**, 302-308; (b) M. Nath, M. Vats and P. Roy, *J. Photochem. Photobiol., B*, 2015, **148**, 88-100; (c) M. A. Girasolo, L. Tesoriere, G. Casella, A. Attanzio, M. L. Capobianco, P. Sabatino, G. Barone, S. Rubino and R. Bonsignore, *Inorg. Chim. Acta*, 2017, 456, 1-8.
- 68 M. -T. Park and S.-J. Lee, *J. Biochem. Mol. Biol.*, 2003, **36**, 60-65.
- 69 C. C. Chou, J. S. Yang, H. S. Lu, S. W. Ip, C. Lo, C. C. Wu, J. P. Lin, N. Y. Tang, J. G. Chung, M. J. Chou, Y. H. Teng and D. R. Chen, *Arch. Pharm. Res.*, 2010, **33**, 1181-1191.

triphenylstannyl((arylimino)methyl)benzoates with selective potency that induce g1 and g2/m cell cycle arrest and trigger apoptosis via ROS in human cervical cancer cells

Tushar S. Basu Baul,^{*a} Imliwati Longkumer, Andrew Duthie,^b Priya Singh,^c Biplob Koch,^{*c} M. Fátima C. Guedes da Silva,^{*d}

Newly synthesized triphenylstannyl 4-((arylimino)methyl)benzoates show enhanced cytotoxicity and excellent selectivity in vitro towards human cervical cancer cells.

